AD-A131 968 AN EXPERIMENTAL AND THEORETICAL STUDY ON CAVITATING PROPELLERS(U) TETRA TECH INC PASADENA CA O FURUYA ET AL. OCT 82 TETRAT-TC-3284-04 1/1

UNCLASSIFIED N00014-79-C-0234 F/G 20/4 NL

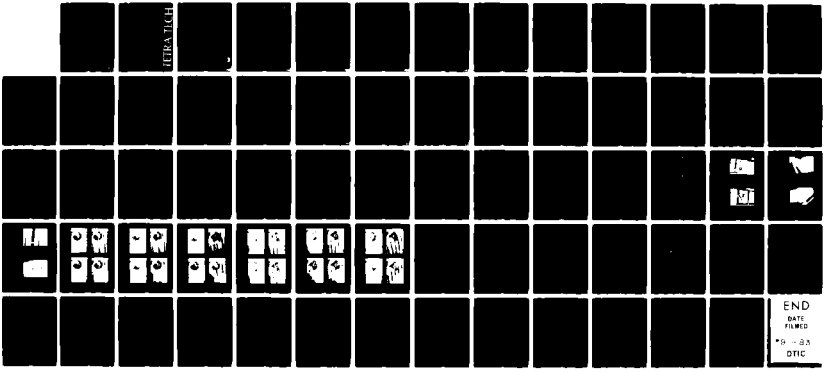

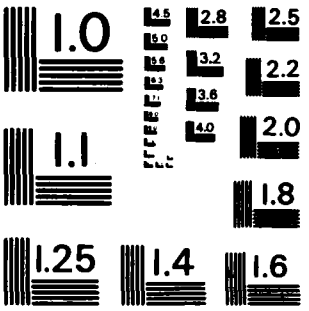

Report No. TC 3284-04
Contract No. N00014-79-C-0234 (GHR Program)

AN EXPERIMENTAL AND THEORETICAL STUDY ON CAVITATING PROPELLERS

by

Okitsugu Furuya
Shin Maekawa

TETRA TECH, INC.
630 N. ROSEMEAD BOULEVARD
PASADENA, CALIFORNIA 91107

Prepared for

DAVID W. TAYLOR NAVAL SHIP
RESEARCH AND DEVELOPMENT CENTER
BETHESDA, MARYLAND 20084

OFFICE OF NAVAL RESEARCH
800 NORTH QUINCY STREET
ARLINGTON, VIRGINIA 22217

OCTOBER 1982

Report No. TC 3284-04
Contract No. N00014-79-C-0234 (GHR Program)

AN EXPERIMENTAL AND THEORETICAL STUDY ON CAVITATING PROPELLERS

by

Okitsugu Furuya
Shin Maekawa

TETRA TECH, INC.
630 N. ROSEMEAD BOULEVARD
PASADENA, CALIFORNIA 91107

Prepared for

DAVID W. TAYLOR NAVAL SHIP
RESEARCH AND DEVELOPMENT CENTER
BETHESDA, MARYLAND 20084

OFFICE OF NAVAL RESEARCH
800 NORTH QUINCY STREET
ARLINGTON, VIRGINIA 22217

OCTOBER 1982

Approved for public release;
distribution unlimited

UNCLASSIFIED

SECURITY CLASSIFICATION OF THIS PAGE (When Data Entered)

REPORT DOCUMENTATION PAGE		READ INSTRUCTIONS BEFORE COMPLETING FORM
1. REPORT NUMBER TC 3284-04	2. GOVT ACCESSION NO.	3. RECIPIENT'S CATALOG NUMBER
4. TITLE (and Subtitle) An Experimental and Theoretical Study on Cavitating Propellers		5. TYPE OF REPORT & PERIOD COVERED Technical Report Nov. 1, 1980 - Oct. 31, 1982 6. PERFORMING ORG. REPORT NUMBER TC 3284-04
7. AUTHOR(s) Okitsugu Furuya Shin Maekawa		8. CONTRACT OR GRANT NUMBER(s) N00014-79-C-0234
9. PERFORMING ORGANIZATION NAME AND ADDRESS TETRA TECH, INC. 630 N. Rosemead Boulevard Pasadena, CA 91107		10. PROGRAM ELEMENT, PROJECT, TASK AREA & WORK UNIT NUMBERS DWTNSR&DC 61153N R02301 SR 023 01 01
11. CONTROLLING OFFICE NAME AND ADDRESS David W. Taylor Naval Ship R&D Center Department of the Navy Bethesda, MD 20084		12. REPORT DATE October 1982 13. NUMBER OF PAGES 65
14. MONITORING AGENCY NAME & ADDRESS(if different from Controlling Office) Office of Naval Research 800 North Quincy Street Arlington, VA 22217		15. SECURITY CLASS. (of this report) Unclassified 15a. DECLASSIFICATION/DOWNGRADING SCHEDULE

16. DISTRIBUTION STATEMENT (of this Report)

Approved for public release; distribution unlimited

17. DISTRIBUTION STATEMENT (of the abstract entered in Block 20, if different from Report)

18. SUPPLEMENTARY NOTES

Sponsored by the Naval Sea Systems Command General Hydrodynamic Research Program and administered by the David W. Taylor Naval Ship R&D Center, Code 1505, Bethesda, MD 20084.

19. KEY WORDS (Continue on reverse side if necessary and identify by block number)

cascade flow	theoretical
supercavitating flow	performance prediction method
partially cavitating flow	supercavitating propellers
experimental	partially cavitating propellers

20. ABSTRACT (Continue on reverse side if necessary and identify by block number)

The original objective of the present work was to develop an analytical tool for predicting the off-design performance of supercavitating propellers over a wide range of operating conditions. Due to the complex nature of the flow phenomena, a lifting line theory simply combined with the two-dimensional supercavitating cascade theory was selected. The results of this simple method provided surprisingly accurate predictions for the performance at fully developed cavitating conditions. It was indicative that the fully-developed, supercavitating propellers had strong cascade effects on their performance, and also that the three-

DD FORM 1 JAN 73 1473 EDITION OF 1 NOV 65 IS OBSOLETE S/N 0102-014-6601

UNCLASSIFIED

SECURITY CLASSIFICATION OF THIS PAGE (When Data Entered)

20. (Cont'd)
dimensional, propeller geometry corrections could properly be made by the lifting-line theory. As was expected, however, the predicted K_T and K_Q curves with this propeller theory showed a significant deviation from experimental data in the range of larger than J_{design} where the partially cavitating conditions are expected to occur. Effort was then made on improving the prediction capability of the above propeller theory at partially cavitating conditions. A new nonlinear partially cavitating cascade theory was then developed to provide a proper 2-D loading basis under such conditions. A slight improvement on the prediction capability of the propeller theory was achieved with the new set of data, but not to a satisfactory extent.

A question was then raised as to the accuracy of the two-dimensional p/c and s/c data, since they had never been compared with experimental data. The main objective of the present phase of the work was, therefore, to conduct the two-dimensional cascade experiments for foils having a practical blade profile shape and then to compare the results with the p/c and s/c cascade theories. One of the typical s/c propeller (Hydronautics' 7607.02) blade profiles was chosen and the experiments were conducted for one-blade, three-blade and five-blade cases. (The results of the one blade experiments were already reported in the paper of Furuya and Maekawa (1982.))

The measured forces and flow observations obtained in these experiments shed a new light on the relationship between the forces and cavitation numbers in small incidence angles. It was found that, due to rather strong cascade effects, the flow configuration was different from what had been expected; instead of having leading edge cavities, base-cavities or double cavities (base-cavity and leading edge cavity) appeared. For the former cases, the lift force coefficients were almost constant over an entire range of cavitation numbers, similar to those of fully-wetted foils. Even for the latter cases, the cavity was very thin so that the lift forces were again flat.

This type of flat lifting force as a function of cavitation number for small incidence angle cases was then used in the propeller program. The calculated results for K_T and K_Q with the new force data successfully correlated with the experimental data, particularly for large J range where the partially cavitating conditions exist.

TABLE OF CONTENTS

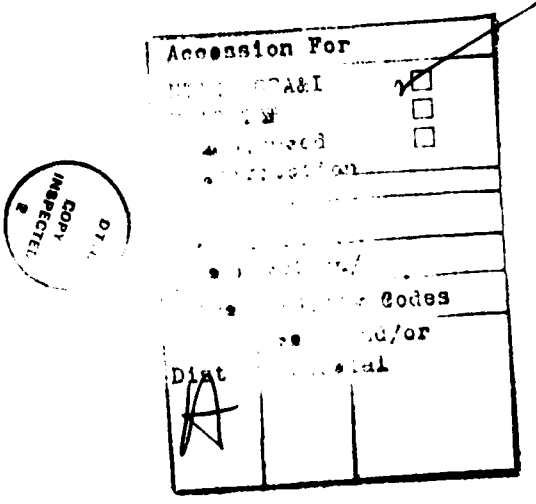

LIST OF FIGURES AND TABLE

List of Figures (Cont'd.)

NOMENCLATURE

A	Area of the plan form = b x c
b	Span of foil
c	Chord length of foil
C_D	Drag coefficient = $\frac{\text{drag force}}{\frac{1}{2}\rho q_1^2 A}$
C_L	Lift coefficient = $\frac{\text{lift force}}{\frac{1}{2}\rho q_1^2 A}$
D	Diameter of propeller
d	Spacing between the two blades in cascade configuration
J	Advance speed = $\frac{V}{nD}$
J_{design}	Designed advance speed
K_T	Thrust coefficient
K_Q	Power coefficient
ℓ_c	Normalized cavity length = $\frac{\text{cavity length}}{c}$
n	Rotational speed of propeller
p_1	Reference static pressure
p_c	Cavity pressure
p_v	Vapor pressure of water
q_1	Tunnel water speed
R	Radius of propeller = D/2
r	Radial distance from the center of propeller
sol	Solidity = d/c
V_a	Ship speed
x	Normalized radial location = r/R
$\bar{x}$	Normalized chord length
α	Angle of incidence
α_e	Effective angle of incidence

Nomenclature (Cont'd)

σ Cavitation number = $\frac{p_1 - p_c}{\frac{1}{2}\rho q_1^2}$

σ_v Vapor cavitation number = $\frac{p_1 - p_v}{\frac{1}{2}\rho q_1^2}$

σ_{V_a} Cavitation number based on ship speed = $\frac{p_1 - p_c}{\frac{1}{2}\rho V_a^2}$

ρ Density of water

1.0 INTRODUCTION

A theoretical method (Furuya (1976)) has recently been developed for predicting the off-design performance of supercavitating propellers, the method being based upon the propeller lifting line theory combined with two-dimensional nonlinear supercavitating cascade theory. The results compared favorably with experimental data, particularly at highly choked conditions, but not quite so for the shorter or partial cavity range. This discrepancy at partially cavitating regime (i.e., for large values of advance speed J) had been expected since the two-dimensional loadings used were not appropriate ones, i.e., those obtained based on the supercavitating cascade configurations. In order to extend the prediction capability of the propeller theory to partially cavitating regions, the two-dimensional nonlinear partially cavitating cascade theory (Furuya and Maekawa (1979) and Furuya (1980a)) was then developed. The results of the p/c cascade theory were incorporated into the above propeller theory. Although the propeller theory with the new set of data added for the partially cavitating regions provided a slight improvement on the prediction of K_T and K_Q values at large J range, they were still considered to be unsatisfactory (see the paper of Furuya (1980b) and also Figure 32)).

A question to be answered then was as to what caused such discrepancy in the performance prediction method, i.e., does the propeller theory itself need improvement or are the two-dimensional basic loading data inappropriate? It was decided then that the first priority should be given to investigate the accuracy of the various two-dimensional (2-D) theories used in the propeller program. The results of these theories had never been properly compared with experiments since the cavitating cascade data were so scarce. These included the works by Numachi (1953) and Wade and Acosta (1966), but none of them used practical blade profile shapes employed by cavitating propellers or pumps.

The objective of the present study was, therefore, to conduct simple yet useful cascade experiments using a practical cascade profile shape and then to compare with the s/c and p/c theoretical data, thus increasing the confidence level for the 2-D loading data used in the propeller performance prediction method.

The cascade blade profile used for the experiments was taken after that of Hydronautics' 7607.02 supercavitating propeller at 50% radial station. Fir , single-foil experiments were conducted, and their re ts (see the paper of Furuya and Maekawa (1982)) represen the extreme case of cascade configuration, i.e., zero so y case.

In this study, four additional foils (we call them "dummy foils") having the same profile as that of the previously tested foil were fabricated to form the cascade configuration. Furthermore, various test-section components including the inserts, movable downstream walls and link system were added to the 2-D test section of the High Speed Water Tunnel (HSWT) at Caltech. The procedure for taking accurate data in cascade experiments is quite tedious due to the necessity of the downstream side wall adjustment. Nevertheless, the data were taken over a wide range of cavitation numbers covering from the fully-wetted, partially cavitating and supercavitating regimes for two different solidity cases, sol = 0.5 and 1.0, i.e., two and four dummy blades used, respectively. These data were then compared with the existing p/c and s/c cascade theories. Based on these force comparisons, as well as the new findings made by the flow observations, a new set of force data were incorporated into the propeller program. With these revised data, the improvement of performance prediction capability for cavitating propellers has been achieved, especially at large J's for which the partially cavitating flow is prevalent.

2.0 EXPERIMENTS

2.1 MODEL

The cross-section profile shape used for the present two-dimensional cascade experiments was taken after Hydronautics 7607.02 s/c propeller at 50% radial station (x = .5). The upper and lower blade off-set data are given in Table 1 (see also Bohn and Altman (1976)). The main reason for choosing the cross-section profile at x = .5 is that the solidity and stagger angle of the propeller there are readily fit with the existing 2-D cascade test section at HSWT of Caltech. This test section was made to have the stagger angle of 45°, whereas that of the Hydronautics 7607.02 s/c propeller at x = .5 is 48.9°. In order to simulate the 2-D cascade flow in the experiment, at least five blades are desired to be used. By choosing the chord of the blade to be reasonably long, i.e., 3.2 inches in this case, the high solidity (sol) such as sol = 1 is achieved. Furthermore, if three-bladed configuration is used, the tests for sol = 0.5, close to that of 7607.02 propeller, i.e., .585, are also carried out. The main portion of propeller blade profile shape consisted of a Tulin's two-term camber ($.2 \leq \bar{x} \leq .8$, where $\bar{x}$ is normalized chord position), with some modification made for the leading edge ($\bar{x} \leq 0.2$) and trailing edge ($\bar{x} \geq 0.8$). The report by Furuya (1978) describes these modifications in detail.

The high lifting forces were expected, particularly at the transient region, i.e., between partially cavitating and fully supercavitating conditions. Therefore, the heat treated stainless steel 17-4PH was used for the center foil (see Figure 1), on which the force measurements were made. The fabrication accuracy of the models was measured and assured to be within $\pm$ 0.002 inches over the entire blade profile (i.e., less than $\pm$ 0.1% chord). The leading edge was specified to be sharp, but in the most physically

possible sense. Four other cascade (dummy) foils were fabricated from 7075-T6 aluminum alloy. These foils were mounted on the lucite window side, opposite from the side on which the center foil is mounted. Since no force measurements were necessary for these foils, pivoted supports were added at the tip of these foils (see Figure 2). Due to this additional structural support (i.e., from a cantilever configuration for the center blade, to a two-point support for the dummy blades), the softer material, easy to fabricate, could be used.

2.2 EXPERIMENTAL SET-UP AND APPARATUS

The High Speed Water Tunnel at the California Institute of Technology is a closed circuit water tunnel, the maximum speed of which can go up to 80 ft/sec. The tunnel pressure can be reduced down to 0.1 atm. More basic features of the water tunnel are discussed at length in Knapp et. al. (1948) and Ward (1976).

For this experiment, the two-dimensional working section, having the dimensions of 30 inches high, 50 inches long, and 6 inches wide, was used. This test section was installed by rotating 90°, thus horizontally, to avoid a large static pressure gradient across the cascade. This is a particular concern for the cascade experiment. Furthermore, a pair of streamlined nozzle inserts was placed, reducing the working section height from 30 inches to 13.6 inches. This set-up provided a freedom of movement for the downstream wall mechanism, which was an absolute necessity for this type of cascade experiment. Due to this freedom, the downstream wall mechanism, attached to the ends of the blocks, could be moved the maximum 10° angle in both directions (see Figure 3).

The main foil was mounted to a base fixture, fitted with a balance port fairing disk (see Figure 2). The force balance

available for the HSWT has a low and a high force range capacity. The low range load cells having a range of ± 200 lbs. lift ± 80 lbs. of drag and ± 300 in-lb. of moment were used for this experiment. The force balance data were stored as the time averaged values in the buffer of the electronic data acquisition system. In this experiment the duration of four seconds was selected to assure the average forces for each force measurement. The force balance data, along with the water tunnel flow velocity, pressure and the downstream wall angles were recorded manually. The accuracy of each cell is within ± 0.25% of the rated load, which is inclusive of all hysteresis, non-linearity, and repeatability.

The dummy foils were installed on the other side of the test section, i.e., opposite from the force balance side. The geometrical stagger angle is 45°, which is fixed due to the constraints of the existing test section. The cylindrical shaft attached to each dummy foil was connected to a link mechanism of cascade blade angle change. Through this link system the angle of all dummy foils can be changed simultaneously (see Figures 4 to 9). The tip clearance, which is the space between the tip of the main foil and side wall, was adjusted to approximately .02 inches at atmospheric pressure. Such a clearance is necessary for avoiding the chance of the main foil's contact against the wall when the tunnel pressure is reduced to the minimum cavitating condition.

2.3 PROCEDURES

The tunnel water velocities were determined through the measured pressure differences across two points at the contracting nozzle section, 85.75 inches and 28.375 inches upstream from the center of the main foil (see Figure 3). The determination of the testing pressure (we call this "reference static pressure") in cascade experiments required

careful thought due to the modification made for the test section and the nature of the testing itself. The reference static pressure for a single-foil testing is usually measured through the pressure hole located 12 inches upstream in this test section. In this cascade experiment, however, this pressure hole is too close to the cascade and it was a concern that the blocking effect of the cascade might have influence on accurate pressure measurements. It was for this reason that the absolute pressure measured at 28.375 inches upstream (instead of 12 inches upstream) was used to determine the reference static pressure for the present experiments. The conversion relationship between the above absolute pressure and the reference static pressure was previously established by Acosta and Wade (1968).

The vapor cavitation number, σ_v, was determined based on the vapor pressure calculated from the measured water temperature. However, for the data presentation, the cavity cavitation number, σ, was used by making appropriate corrections on σ_v. Detailed descriptions regarding such corrections will be given in the following section.

The procedure of conducting cavitating cascade experiments was identical to that for single foil cases except for the tedious downstream wall angle adjustments. After the cascade foils were set at a desired angle, the water velocity was increased to a preset value, 25 ft/sec. The downstream wall angle was fixed at any preselected positive value for the first trial. The static pressure of the text section was then gradually reduced until the cavity on the foil appeared and finally the tunnel was choked. The data points were selectd at various pressure points for various cavity lengths. The lift and drag data along with the photographs were recorded at each datum point. However, these measured data might not be accurate since the downstream wall angle

was arbitrarily selected for the first run. It means that the pressure field generated immediately downstream of the cascade was not guaranteed to be uniform across the cascade blades. In order to achieve the uniform pressure field, the measured lifting force should satisfy the momentum equation in the direction normal to the effective average flow angle. This fact indicates the requirement for iterative procedure in adjusting the downstream wall angle. In our experimental procedure, therefore, based on the measured lifting force and by applying the momentum equation, the downstream wall angle was re-calculated on the spot. With the revised downstream wall angle and the same angle of incidence and the water velocity, the test was run again and the forces were recorded. This iterative procedure was repeated until the downstream wall angle and thus the measured forces became converged. The maximum of five iterations was necessary for obtaining such convergent results. All the force data taken were averaged over 4 seconds, displayed on a LED numerical display of the data acquisition system, and recorded manually on the data sheets along with the water velocity, reference static pressure, and the geometrical set up.

Due to the various accessories mounted around the cascade (see Figures 4 to 9), only obliquely viewed photographs were taken by using two strobe lights. The duration of the lights was approximately 10 microseconds.

2.4 DATA REDUCTION

The cavitation number based on the cavity pressure is defined

$$\sigma = \frac{p_1 - p_c}{\frac{1}{2}\rho q_1^2}$$

where p_1 is the reference static pressure, p_c is the cavity pressure, ρ is the density of water and q_1 is the velocity

of the water at the test section. On the other hand, the cavitation number based on the water vapor pressure is defined

$$\sigma_v = \frac{p_1 - p_v}{\frac{1}{2}\rho q_1^2}$$

where p_v is the vapor pressure of water at the temperature during the experiment. Since the cavity pressure measurements were not made in these experiments, it was decided to make corrections on σ_v's to obtain σ's. The correlation between σ and σ_v was presented in Kermeen (1956) and Wade and Acosta (1966) and this was used for the present purpose. Due to the lack of correction data in the region of $\sigma > 1.5$, the cavitation numbers are left uncorrected in such region. It must be mentioned, however, that the use of uncorrected cavitation numbers for large σ's will not greatly affect the force data presentation since the forces there are relatively constant as a function of σ.

The measured forces were normalized

$$C_L = \frac{\text{Lift}}{\frac{1}{2}\rho q_1^2 A}$$

$$C_D = \frac{\text{Drag}}{\frac{1}{2}\rho q_1^2 A}$$

where A is the plan form area of the model. First it was found in the no-flow, static pressure change runs that the influence of the pressure change of the tunnel on the force balance reading was negligibly small. The main corrections necessary for the measured forces were for the viscous drag forces acting on the model and the fairing disk. Over the tested water velocity range, the boundary layer was considered to be predominantly turbulent. The viscous drags on the model and fairing disk were estimated by Prandtl's tur-

bulent boundary layer equation. The wetted areas for this correction needed to be varied, depending on the flow conditions, i.e., fully wetted, partially cavitating, or supercavitating.

3.0 RESULTS OF CAVITATING CASCADE EXPERIMENTS

3.1 FLOW OBSERVATIONS

Figures 10 to 12 show the flow patterns at α = 4°, 6°, and 8°, respectively for the case of sol = .5 (three-bladed configuration). For the cases of α = 4° and 6°, it is seen that the base cavities appeared almost simultaneously with the leading edge cavities. For α = 8° case, however, first the leading edge cavity appeared, followed by the base cavities with an additional substantial decrease in the tunnel pressure. For all three cases, the cavities, one from the leading edge and the other from the trailing edge, merged together with a further decrease in the tunnel pressure. The merging of the two cavities usually took place as soon as the leading edge cavity grew .5 ~ .6 of the chord length. Once the cavity extended beyond the chord, e.g., to 1.2 chord lengths, it was observed relatively stable. For all angles of incidence, the cavity surfaces were bubbly for short to medium cavity lengths (0 ~ 2 chord lengths), while clear sheet-like cavities were observed as the cavity length further increased.

Figures 13 to 15 show the flow patterns at α = 4°, 6°, and 8°, respectively for the case of the sol = 1.0 (five-bladed configuration). The flow patterns observed in these high solidity cases are essentially similar to those of sol = .5 except for the fact that the base and leading-edge cavities took place at pressures different from those at sol = .5. Generally speaking, the cascade effect was much more prevalent at this high solidity case. For example, the base and leading-edge cavities did not take place until much lower cavitation numbers (than for the case of sol = .5) were reached. It means that the high pressure field generated by the pressure side of the adjacent blade prevented the cavitation from occurring at an early stage of pressure reduction. In Figures 16 to 21, the cavitation numbers at which the base and leading-edge cavities took place are indicated.

3.2 FORCE COEFFICIENTS

Figures 16 to 18 show the lift coefficients as a function of cavitation number for α = 4°, 6°, and 8°, respectively. Two solidity cases, sol = 0.5 and 1.0, are shown along with the results of the single foil experiment (i.e., sol = 0) obtained in the previous study (see the paper of Furuya and Maekawa (1982)).

The forces at α = 4°, 6°, and 8° all provided a consistent pattern going from the fully wetted, partially cavitating (p/c) to supercavitating (s/c) conditions. Peak values were observed at the transition region, i.e., existing between p/c and s/c conditions for all α's and sol's, except for the case of α = 4° and sol = 1. For this small α and large solidity case, the cascade effect appeared to be very strong; the observed cavity was fairly thin and thus the usual camber effect generated by the upper cavity boundary was minimum.

Attention must also be paid to the existence of multiple force values at these transition regions, which are marked by the shaded area in those figures. It was observed in the experiments that the flow became quite unstable as the cavity length approached the chord length. After the last stable partially cavitating point was measured, the tunnel pressure was further reduced. With a slight decrease in pressure the cavity extended to the chord length or slightly longer. But after shedding cavity bubbles downstream, it shrank back to a shorter length. The duration of the cavity staying at either long or short length was about 5 to 10 seconds, but with relatively fast transition time from one condition to the other, e.g., about 1 second. This self-oscillatory motion continued and could not be suppressed by adjusting the tunnel pressure and/or velocity. The

manometers' readings for the tunnel pressure and velocity also showed continuous fluctuations, although they were of small quantity. Therefore, depending upon where the cavity end was found, the measured forces varied significantly even for the same pressure and velocity readings as are shown in the figures. It was, however, clearly indicated by careful correlations between the measured forces and photographs that smaller forces were always recorded for short cavities, and larger forces for the cavity length close to the chord. Although this multi-valuedness in forces and cavity lengths seems to be the nature of the flow, the larger values of measured forces should represent the right forces at such cavitation numbers. It should be pointed out that this type of oscillatory behavior in the cavity flow was hardly observed in the single foil experiments (see the report of Furuya and Maekawa (1982)), and thus is characterized as a specific nature for the cavitating cascade flows, coupled with the closed-circuit water tunnel dynamics.

The effect of solidity, partially mentioned above, can readily be seen from these lift-curves at all α's. See the lift coefficients at the fully wetted region; those of sol = .5 are about half the lift forces at sol = 0 and those at sol = 1.0 are further reduced to half the lift forces of sol = .5.

The nonlinear supercavitating and partially cavitating cascade theories (see the papers of Furuya (1975) and Furuya and Maekawa (1979)) were used for comparison with the experimental data, along with the results of the previously developed nonlinear single foil theories. These are shown in Figures 16 through 21. The computations were possible only for the lower solidity case (sol = .5) due to the increased inaccuracy in numerical iterative procedure for large solidity cases such as sol = 1.0.

The supercavitating theories for the lift coefficients correlated well with the experiment, especially for medium-length cavity cases, but it slightly over-predicted for the smaller cavitation number, where the cavity is long. This discrepancy at low cavitation number may possibly be caused by the inaccuracy of the water velocity measurement around the choking condition. Once such a choking condition occurred, it was found that the control of both tunnel pressure and velocity to the desired values became extremely difficult.

It must also be pointed out that the slope of lift curves increased with decrease in the incidence angles. It is interesting to note, also, that this trend is not only shown by the measured data, but is well predicted by the nonlinear s/c cascade and single foil theories.

The overall correlations of the partially cavitating theories with the experiment for the lift coefficients are also good, except for a large incidence angle, $\alpha = 8°$. At $\alpha = 8°$, the theory overestimates the lift coefficients. It seems that this overprediction may be caused by the theory's inability to determine the partial cavity length accurately. This fact will be seen in the comparison curves for the cavity length vs. cavitation number, as is shown in Figures 22 to 24. For low incidence angle cases, i.e., $\alpha = 4°$ and $6°$, the theory agrees well with the experiments, whereas for the higher incidence angle, $\alpha = 8°$, the correlation is poor. It must be mentioned, however, that the theory's inability of accurately determining the lift coefficients at high incidence angles may not affect the capability of the off-design performance prediction method for cavitating propellers and pumps. The reason is that the partially cavitating condition in such machinery always occurs at very small incidence angles in each blade component.

In the transition regions the inherent oscillatory cavitations were observed during the experiments, as has been described earlier. It is a well-known fact that this type of oscillation also manifests itself in cavity flow theories. The numerical iterative procedure in the presently-used partially cavitating theories failed to converge as the cavity length approached the chord length, indicating the abnormality at such conditions.

A problem now arises as to what values of forces should be used at such transition points in the performance prediction methods. In the method used for predicting the performance of cavitating propellers, the two curves, obtained by the s/c theory and p/c theory, are connected wherever they meet. Again, it must be mentioned that the appearance of such a transition region in real fluid machinery is rare except for, e.g., cavitating propellers; under a certain condition the propeller blade tip area is supercavitated and the blade root area is partially cavitated so that somewhere in between there exists a transition condition where the cavity length is equal to the chord length. It is interesting to note also that such a local transition condition existing in the fluid machinery is rather stable.

For the prediction of the drag coefficients, the s/c theory compared well with the experiments, but in the partially cavitating regime the p/c cascade theory considerably underpredicted the drag forces. This discrepancy seemed to stem from the fact that the base cavity was observed in the experiments, whereas the p/c cascade theory was formulated without the existence of the base cavity. The existence of such base cavity in the experiments also presented a specific characteristic in that the peak values of drag forces always correlated with the inception of base cavity, as is marked in Figures 19 to 21.

3.3 CAVITY LENGTH

Figures 22 to 24 show the cavity length vs. cavitation number for α = 4°, 6°, and 8°, respectively. Each figure contains three different solidity cases, i.e., 0, 0.5 and 1.0, which are compared with the theoretical results. The cavity length measurements in these experiments were made through photographs so that the accuracy levels were considered to be $\pm$ 5% of the measured values. As is seen from these comparisons, the s/c and p/c cascade theories predicted their trends well, particularly for α = 4° and 6°. For the larger incidence angle case, α = 8°, however, the s/c cascade theory has a tendency to underpredict, whereas the p/c cascade theory tends to overpredict the cavity length. As has been explained earlier, this may have caused the inaccurate theoretical prediction of force coefficients at α = 8°.

4.0 OFF DESIGN PERFORMANCE PREDICTION OF SUPERCAVITATING PROPELLERS

4.1 PREPARATION OF SECTIONAL DATA

In light of the experimental observations and force measurements made, the force coefficients for the Hydronautics' 7607.02 propeller used in the off-design performance prediction method (Furuya and Maekawa (1979)) were re-examined. The force coefficients at the supercavitating conditions were found to be relatively accurate and correlate well with the theory for all incidence angle cases. On the other hand, in the partially cavitating regions the p/c theory predicted the force coefficients well only for moderate flow incidence angles such as α = 4° 6°. At the smaller incidence angles such as α = 2°, however, it was learned from the flow observations that not only the leading edge cavity, but also the base cavity existed, as has been explained earlier. A further decrease in incidence angle (i.e., to α = 0°), suppressed the leading edge cavity totally and only the base cavity continued to exist as the tunnel pressure reduced. Evidence for supporting this fact is given in Figure 25, which was obtained from the previously conducted single foil experiments (Furuya and Maekawa (1982)). In this figure it is seen that the lift coefficients are flat over a complete range of cavitation number since no leading-edge cavity existed and, therefore, no effective camber increase took place.

When the off-design performance of 7607.02 propeller was calculated in the previous study of Furuya and Maekawa (1979), the cavity flow pattern change just described above was never taken into consideration. For all incidence angles and cavitation numbers, the leading edge cavities, both for partial or supercavitating condition, were assumed.

In order to incorporate more accurate force coefficients reflecting the experimental findings into the propeller

program, the numerical results of the supercavitating cascade theory were carefully re-examined, particularly for the upper cavity profile shapes. It has been discovered that, at the locations of propeller blades near the hub where the solidity is high, the calculated upper cavity boundaries sometimes interfere with the blade boundary, when the flow incidence angles are small. For example, at 50% radial position of blade (sol = .585) and $\alpha = 0°$, it was found that the cavity never cleared the foil surface at all ranges of cavitation numbers.

It means that the force coefficients calculated by the theory under the assumption of the existence of supercavitation are totally irrelevant. Incidentally, in the propeller program, the force coefficients at very small incidence angles such as $\alpha = 0°$ to $2°$ were not provided as the calculated results, but were extrapolated from the forces of larger incidences angles. Those forces were obtained from the s/c or p/c cascade theories, depending upon the cavitation number. It must be noted that the extrapolated forces belong to the class of s/c or p/c conditions having the leading-edge cavities. This is apparently an erroneous selection of force coefficients since the actual flow conditions are of rather base-cavity or double-cavity type.

Since cascade theories with base-cavity or double-cavity have not been developed to date, the forces at such conditions should be obtained in some alternative ways. It was found that the force coefficients at short cavity cases even with base cavities are very close to those at the fully wetted condition, as can be seen in Figures 16 through 18. Therefore, the lift coefficients, at moderate angles of incidence with short cavity lengths, were used to extrapolate those at the small angles of incidence. This new extrapolation method was introduced here based upon the

experimental findings that rather flat lift coefficients over an entire range of cavitation numbers were obtained for the small incidence angle cases (due to the existence of base cavities). Figure 26 shows such extrapolations for x = 0.5, 0.6 and 0.7 (radial location) of Hydronautics' 7607.02 propeller, respectively. Those extrapolated lift coefficients were incorporated into the existing input data set for the propeller program, SCPROP2. Figures 27 through 31 show the revised sectional lift coefficients as a function of cavitation number for the various angles of incidence.

Generally speaking, it was found that the extrapolated forces previously used were much larger than those of base-cavity or double-cavity cases. It seems for this reason that the performance prediction method had previously overpredicted the propeller thrust and torque coefficients at large J regions where the partially cavitating condition is prevalent.

4.2 APPLICATION OF THE REVISED CASCADE DATA TO A CAVITATING PROPELLER PROGRAM (SCPROP2)

The objective of the present work was to improve the prediction capability of the propeller program developed by Furuya (1976) and improved by Furuya and Maekawa (1979), particularly for large J range where the partial cavitating conditions are prevalent. For the propeller program here the improved sectional data of the cascade flow at the low angles of incidence were implemented.

With these new data used, calculations were made for K_T, K_Q and η at a cavitation number, σ_{Va} = .343 for the Hydronautics' 7607.02 propeller (σ_{Va} is the cavitation number based on the ship advance speed without considering the wake effect). The results are shown in Figure 33 in comparison with the experimental data of Peck (1977) and Bohn (1977). The new calculations provided a significant

improvement over the previously predicted results, particularly in the area of partially cavitating conditions (i.e., $J = 1.05 \sim 1.2$).

It must be mentioned, however, that discontinuities in these curves appeared at around $J = 1.05$. It means that these force coefficients, K_T and K_Q, calculated by starting from a small J did not match with those started from a large J.* This discontinuity problem seemed to occur since flow patterns entirely changed at such a J, i.e., from supercavitating condition to partially cavitating condition. A careful observation of the experimental results by Peck (1977) and Bohn (1977) also shows a trend, i.e., slope change in K_T and K_Q curves at $J \sim 1.05$, although the experimental data do not show any discontinuity.

Figure 34 shows detailed information obtained by SCPROP2, i.e., the local effective incidence angles as a function of spanwise location x at various J's. As can be seen from the figure, the local effective angles of incidence show erratic movements between $J = 1.00$ and 1.05 at $x = .5$ and .6 locations.

Figure 35 shows the detailed comparison of the cavity envelopes on the propeller blade computed by SCPROP2 in comparison with the observation made by Bohn (1977) at the various J's. Generally, the observed cavity lengths are shorter than those calculated by SCPROP2. Furthermore, the experimental observation showed the base cavities, whereas our results could not present any base cavity profiles since SCPROP2 did not actually include the detailed base cavity information as has been discussed in the previous section.

*Note: The propeller performance prediction program uses an iterative method in which the starting values for local flow incidence angles are necessary. Usually, the previously calculated values at a J-value are used to calculate K_T, K_Q, etc., at another value of J (see the paper of Furuya (1980) for more details).

5.0 CONCLUSIONS

The original objective of the present work was to develop an analytical tool for predicting the off-design performance of supercavitating propellers over a wide range of operating conditions. Due to the complex nature of the flow phenomena, a lifting line theory simply combined with the two-dimensional supercavitating cascade theory was selected. The results of this simple method provided surprisingly accurate predictions for the performance at fully developed cavitating conditions. It was indicative that the fully-developed, supercavitating propellers had strong cascade effects on their performance, and also that the three-dimensional, propeller geometry corrections could properly be made by the lifting-line theory.

As had been expected, however, the predicted K_T and K_Q curves with this propeller theory showed a significant deviation from experimental data in the range of J's larger than J_{design}, where the partially cavitating conditions are expected to occur. Effort was then made on improving the prediction capability of the above propeller theory at partially cavitating conditions. A new nonlinear partially cavitating cascade theory was then developed to provide a proper 2-D loading basis under such conditions. A slight improvement on the prediction capability of the propeller theory was achieved with the new set of data, but not to a satisfactory extent.

A question was then raised as to the accuracy of the two-dimensional p/c and s/c data, since they had never been compared with experimental data. The main objective of the present phase of the work was, therefore, to conduct the two-dimensional cascade experiments for foils having a practical blade profile shape and then to compare the results with the p/c and s/c cascade theories. One of the typical s/c propeller (Hydronautics' 7607.02) blade profiles

was chosen and the experiments were conducted for one-blade, three-blade and five-blade cases. (The results of the one blade experiments were already reported in the paper of Furuya and Maekawa (1982).)

The measured forces and flow observations obtained in these experiments shed a new light on the relationship between the forces and cavitation numbers in small incidence angles. It was found that, due to rather strong cascade effects, the flow configuration was different from what had been expected; instead of having leading edge cavities, base-cavities or double cavities (base-cavity and leading edge cavity) appeared. For the former cases, the lift force coefficients were almost constant over an entire range of cavitation numbers, similar to those of fully-wetted foils. Even for the latter cases, the cavity was very thin so that the lift forces were again flat.

This type of flat lifting force as a function of cavitation number for small incidence angle cases was then used in the propeller program. The calculated results for K_T and K_Q with the new force data successfully correlated with the experimental data, particularly for large J range where the partially cavitating conditions exist.

Based on the present study the following conclusions will be drawn:

1) The supercavitating and partially cavitating cascade theories of Furuya (1975) and Furuya and Maekawa (1979) predict the force coefficients well, particularly under moderate loading conditions, so that they can be comfortably used for design and analysis of supercavitating and partially cavitating propellers and pumps.

2) For the cases of small incidence angles in combination with high solidity, these theories must be

carefully used, in that sometimes the calculated cavity boundary interferes with the solid boundary of the blade, indicating the existence of different types of cavities, such as base-cavities or double-cavities.

3) The cascade effect is quite eminent in high solidity configuration; this effect should be well taken into account in design work since the cavitation inception condition, as well as the cavitation pattern, may be totally different from those of low solidity or single foil cases (generally speaking, the cavitation inception is delayed and the effect of incidence angle is mitigated).

4) In the present cascade experiments, unstable cavities were observed in the transition region, which existed between the supercavitating and partially cavitating conditions. Such instabilities never existed in the single foil experiments and thus this instability phenomena in the cascade experiments were considered as inherent characteristics for the cascade flow coupled with the closed-circuit water tunnel dynamics.

5) The lift coefficient curves for the cascade having base-cavities or very thin leading-edge cavities were found to be almost flat over an entire range of cavitation number, the fact being similar to the cases of fulled-wetted cascade flow.

6) The performance prediction method for cavitating propellers, initially developed by Furuya (1976) and improved as results of the present study, provided a good correlation with experimental data over a wide range of advance speed, covering from highly choked supercavitating conditions to partially cavitating conditions.

7) It is interesting to observe that the predicted K_T and K_Q curves clearly identified the transition region at which the propeller flow configuration shifts from supercavitating to partially cavitating condition, or vice versa. Incidentally, the experimental data of Peck (1977) and Bohn (1977) also showed rather distinct change in slope for K_T and K_Q curves, indicating such flow transition.

8) In relation to the above fact, it is noticed that the thrust coefficient starts increasing as J further goes into the very short supercavitating or even partially cavitating regions. Consequently, the efficiency substantially increases. It must be pointed out, however, that the shift of design J value towards such region in order to gain a high efficiency may not be advisable in design procedure. The reason is that such a design will increase the risk for propellers to be operated at unstable short s/c conditions or even at p/c conditions.

9) In the report of Peck (1977), the test results of two propellers, 4698 (equivalent to 7607.02) and 4699, designed for the same design specifications but by two different parties independently, showed that the latter had much higher efficiency, 77% than the former, 52%. Judgment for the superiority of design methods should not be made simply based on the efficiencies. The same report showed the measured J = 1.13 for 4699, whereas J for 4698 is .96, thus the former taking the risks mentioned above. As a matter of fact, in the same report the sketch based on the visual observation indicates that the cavity envelope of 4699 at J = 1.13 is extremely short as a supercavitating condition, almost closed at the blade trailing edge.

6.0 REFERENCES

Acosta, A.J. and Wade, R.B., 1968, Experimental study of cavitating hydrofoils in cascade. *Hydrodynamics Lab. Report NGR05-002-059 of California Institute of Technology.*

Bohn, J.C., 1977, Model tests of a supercavitating propeller designed for a hydrofoil ship. *Hydronautics Reports, 7607.59, August.*

Bohn, J.C. and Altman, R., 1976, Two supercavitating propeller designs for hydrofoil ships. *Hydronautics Technical Report 7607.01.1.*

Furuya, O., 1975, Exact supercavitating cascade theory. *Journal of Fluid Engineering, ASME. Vol. 97, December, 419-429.*

Furuya, O., 1976, Development of an off-design predictive method for supercavitating propeller performance. *Tetra Tech Report TC-676.*

Furuya, O., 1978, Part I: Calculations of the off-design performance for Hydronautics' SC Propeller, Part II: Theory improvement for computer code "SCSCREW". *Tetra Tech Report TC 3913 and 3239.*

Furuya, O., and Maekawa, S., 1979, Partially cavitating cascade theories and their application to cavitating propeller flows. *Tetra Tech Report TC-3284-01.*

Furuya, O., 1980a, Nonlinear theory for partially cavitating cascade flows. *10th Symposium of IAHR, Tokyo, Japan, 221-241.*

Furuya, O., 1980b, Off-design prediction method for supercavitating propellers. *Thirteenth Symposium, Naval Hydrodynamics of ONR, Tokyo, Japan, 133-158.*

Furuya, O., and Maekawa, S., 1982, A theoretical and experimental study on cavitating foils over a full range of cavitation numbers. *11th Symposium of IAHR, Amsterdam, Netherlands, paper #4*

Kermeen, R.W., 1956, Water tunnel tests of NACA 4412 and Walchner profile 7 hydrofoils in noncavitating and cavitating flows. *Hydrodynamics Lab. Report No. 47.5 of the California Institute of Technology.*

Knapp, R.T., Levy, J., O'Neill, J.P. and Brown, F.B., 1948, The hydrodynamics laboratory of the California Institute of Technology. *Transactions of the ASME, Vol. 70.*

Numachi, F., 1953, Cavitation tests on hydrofoils in hydrofoils in cascade. *Transactions of the ASME, Vol. 75, October, 1257-1269.*

Peck, J.G., 1977, Cavitation performance characteristics of supercavitating propellers 4698 and 4699. *DWTNSRDC Ship Performance Department, Department Report SPD-680-02, December.*

Wade, R.B. and Acosta, A.J., 1966, Experimental observations on the flow past a plano-convex hydrofoil. *Transactions of the ASME, J. of Basic Engineering, Series O, Vol. 88, p. 273.*

Wade, R.B. and Acosta, A.J., 1967, Investigation of cavitating cascade. *ASME, Journal of Basic Engineering, December, 693-706.*

Ward, T.M., 1976, The hydrodynamics laboratory at the California Institute of Technology--1976. *Transactions of the ASME, J. of Fluids Engineering, December, 740-748.*

TABLE 1

Blade section offsets of
Hydronautics' 7607.02 supercavitating propeller at x = .5

STATION		OFFSET INCHES		TOTAL THICKNESS	
Percent Chord	Distance from L.E.	Upper (Back)	Lower Face	Inches	Percent
0	0	0	0	0	0
5	.160	.023	-.009	.032	1.0
10	.320	.039	-.016	.055	1.7
15	.480	.051	-.023	.074	2.3
20	.640	.060	-.029	.089	2.8
25	.800	.068	-.036	.104	3.3
30	.960	.075	-.044	.119	3.7
35	1.120	.082	-.052	.134	4.2
40	1.280	.088	-.060	.148	4.6
45	1.440	.093	-.068	.161	5.0
50	1.600	.098	-.077	.175	5.5
55	1.760	.103	-.086	.189	5.9
60	1.920	.107	-.096	.203	6.3
65	2.080	.110	-.107	.217	6.8
70	2.240	.114	-.117	.231	7.2
75	2.400	.116	-.129	.245	7.7
80	2.560	.119	-.140	.259	8.1
85	2.720	.120	-.153	.273	8.5
90	2.880	.122	-.167	.289	9.0
95	3.040	.122	-.183	.305	9.5
100	3.200	.121	-.202	.323	10.1

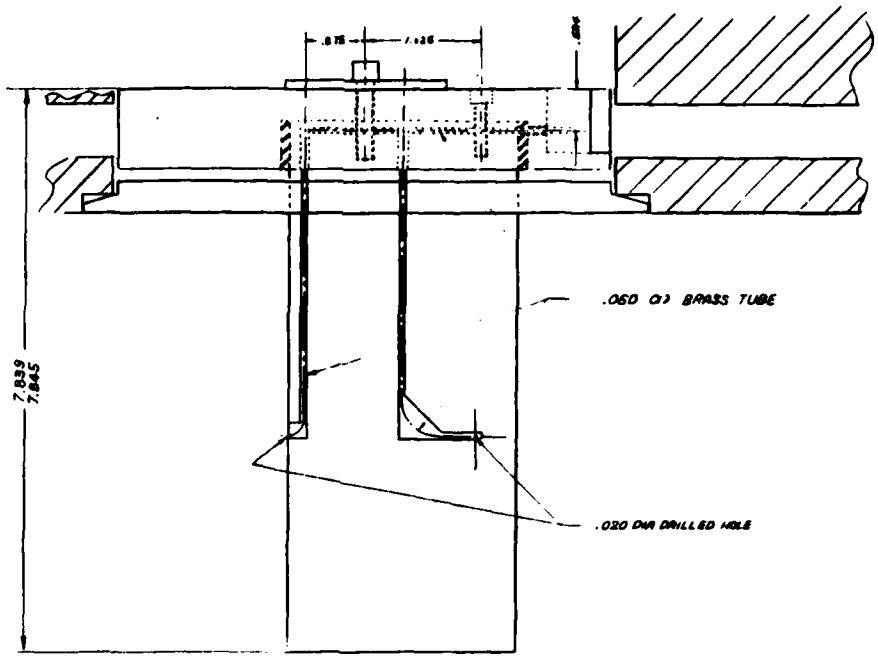

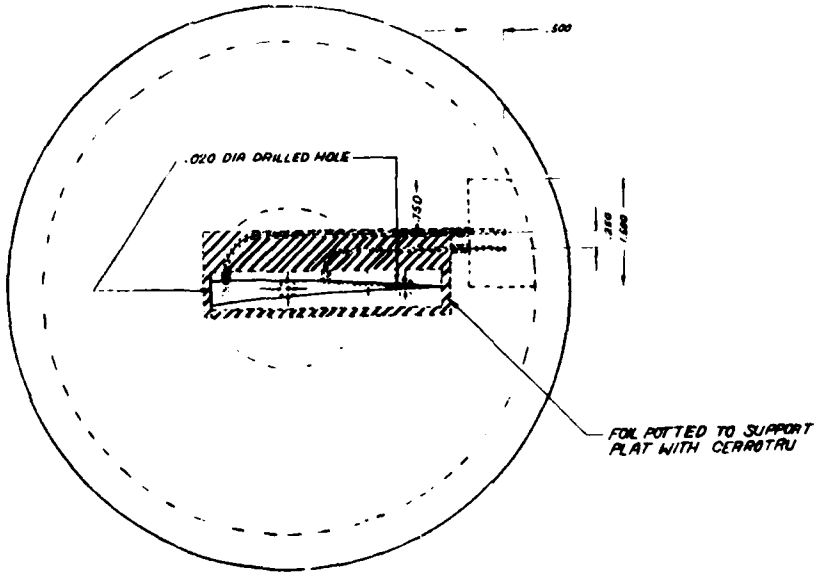

FIGURE 1
Main foil set-up to the tunnel wall

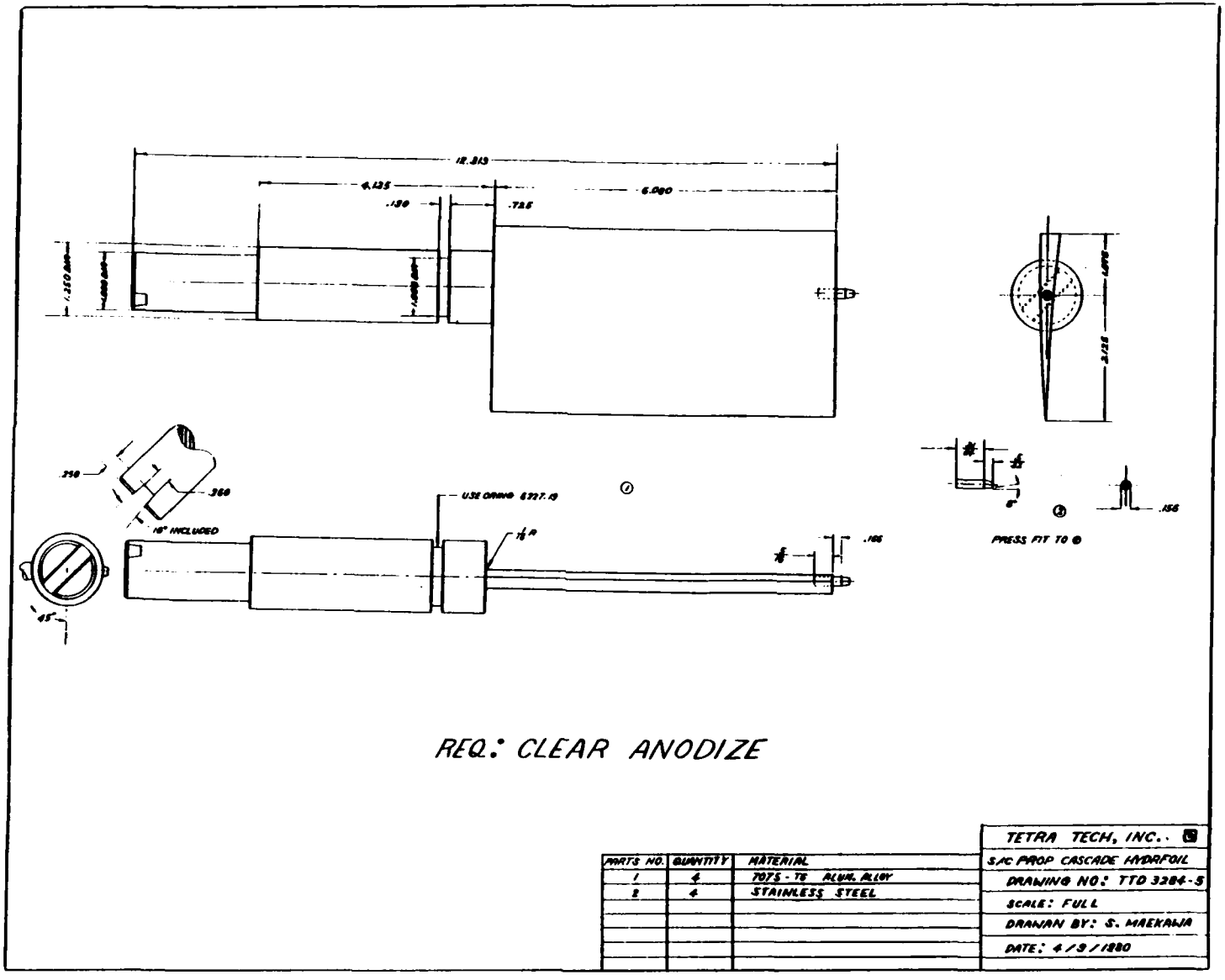

FIGURE 2

Configuration of cascade foils

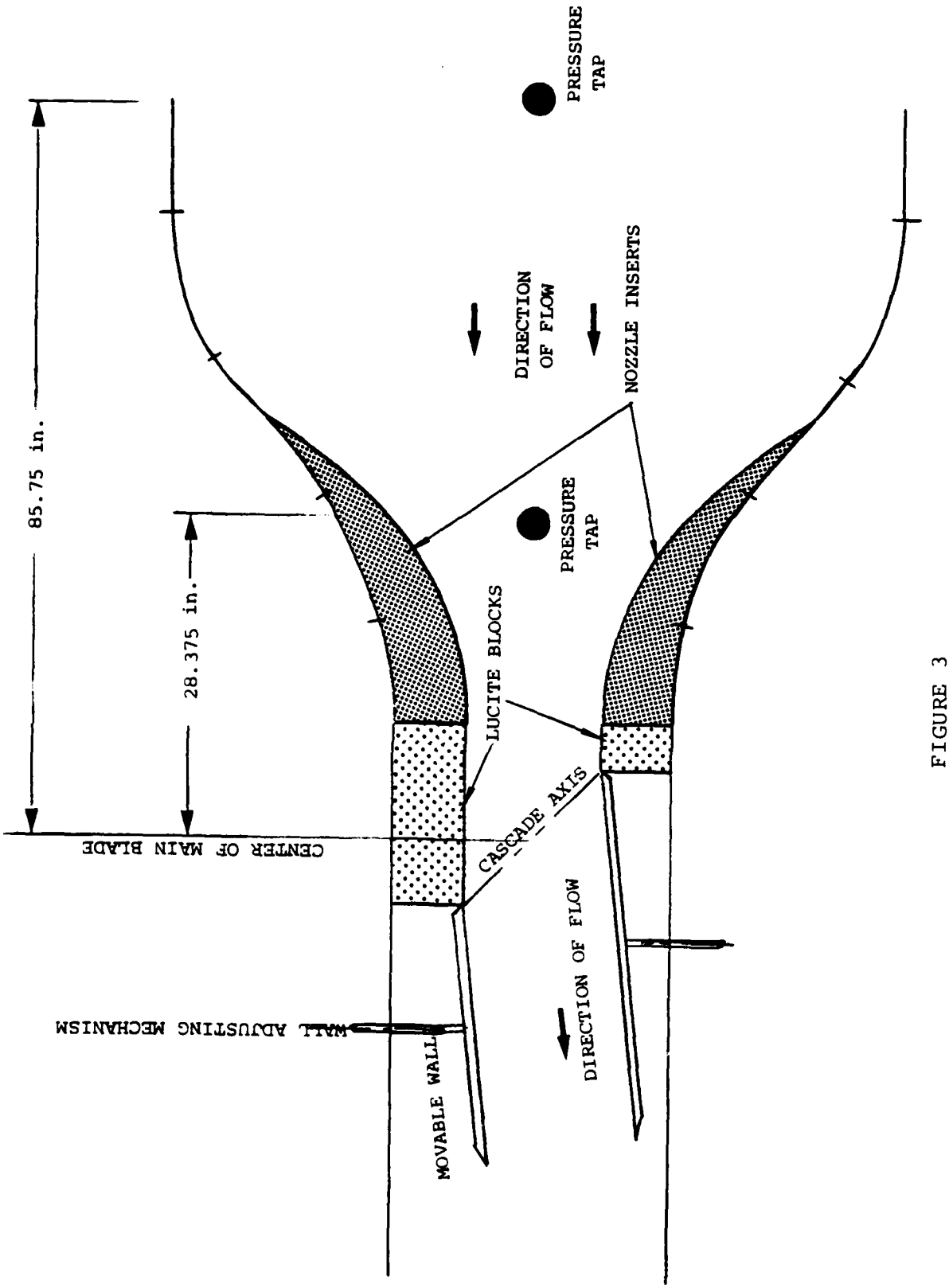

FIGURE 3
Schematic of cascade set-up

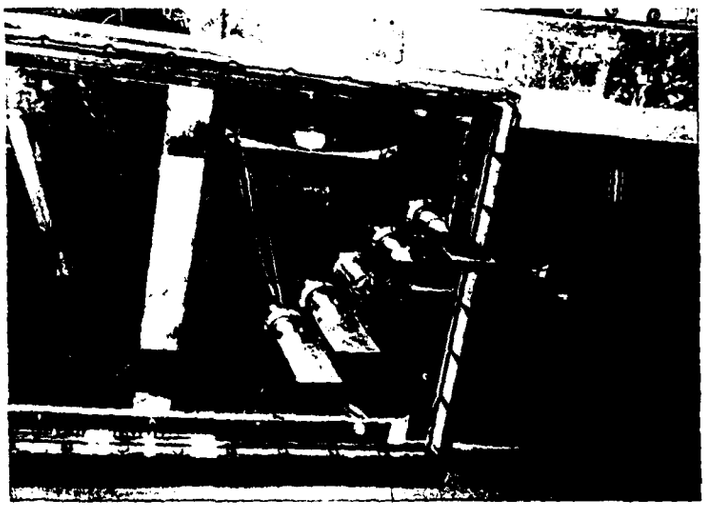

FIGURE 4

Cascade foils mounted through top window

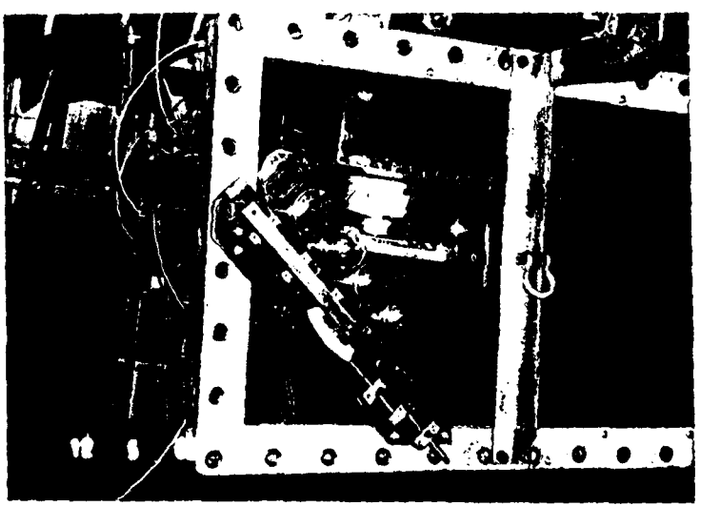

FIGURE 5

Cascade angle changing mechanism

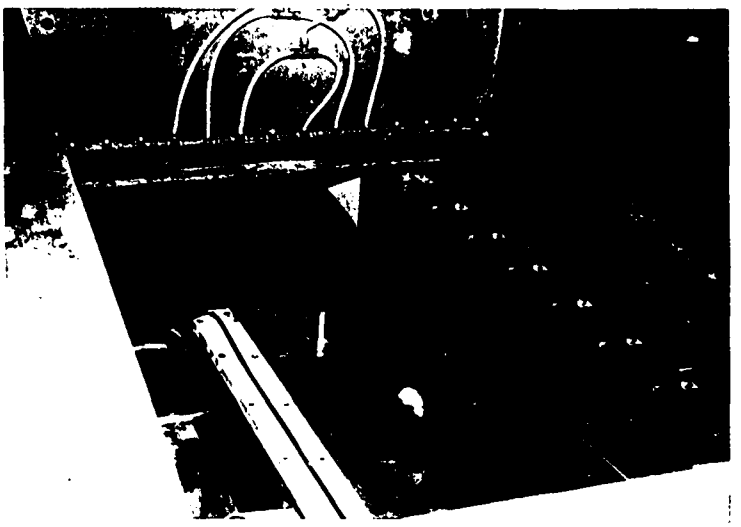

FIGURE 6

View of blocks, center foil,
and downstream walls

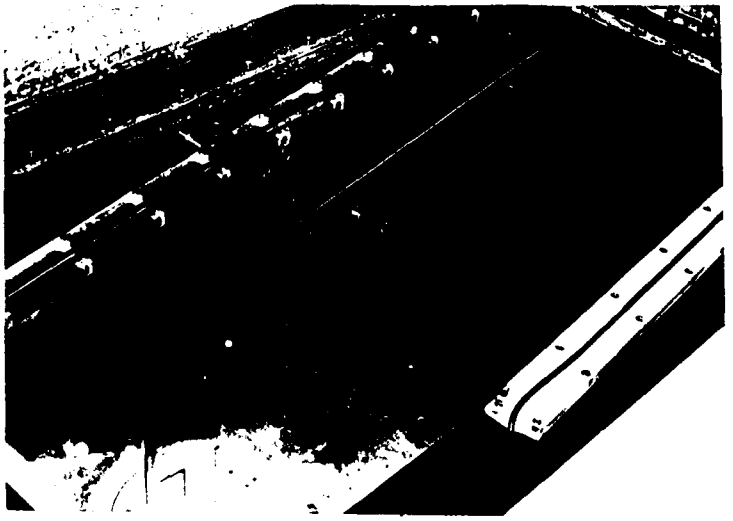

FIGURE 7

View of downstream wall

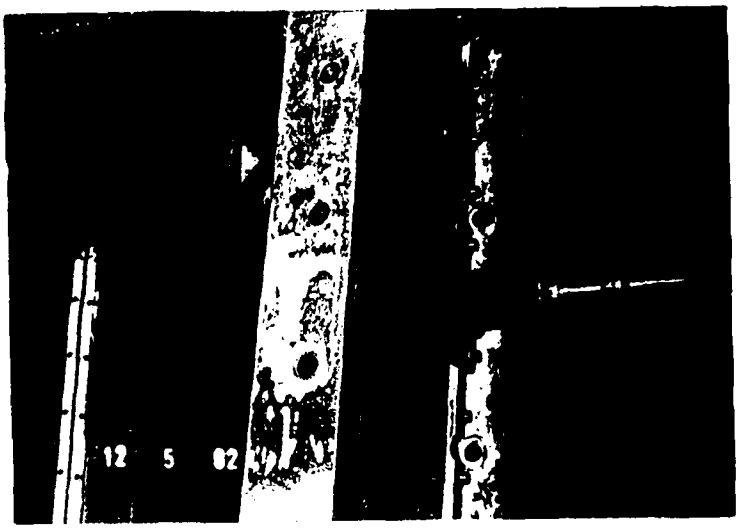

FIGURE 8

View of test section with downstream wall actuating mechanism

FIGURE 9

View of downstream wall actuating mechanism

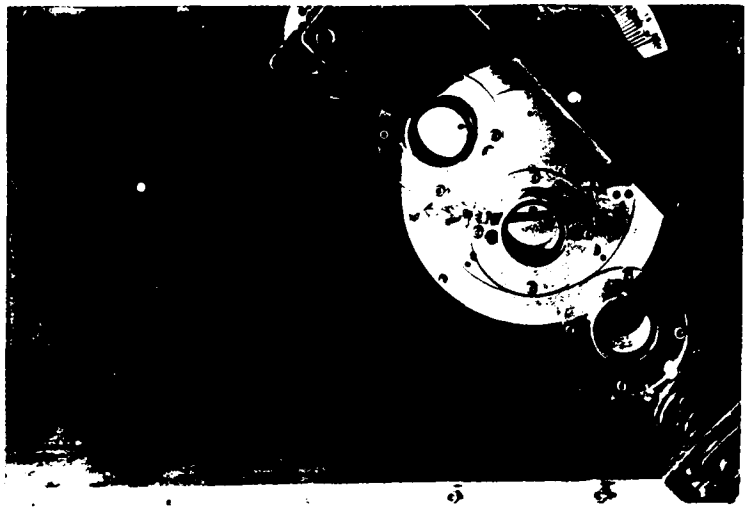

(a) σ = .53

(b) σ = .33

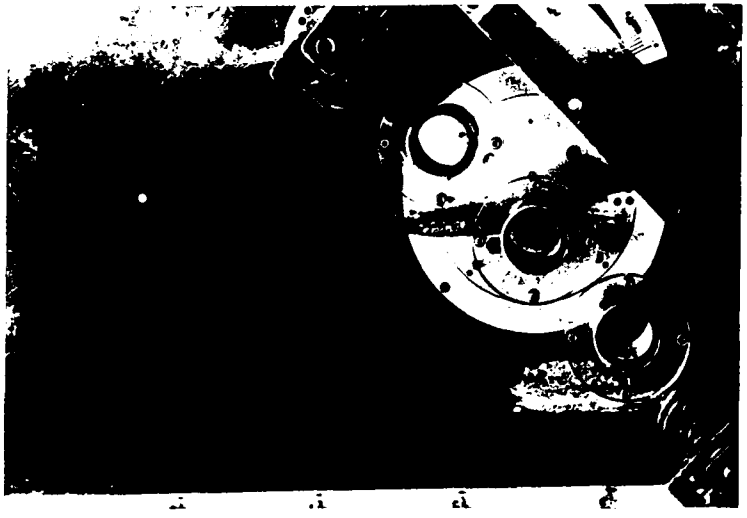

(c) σ = .20

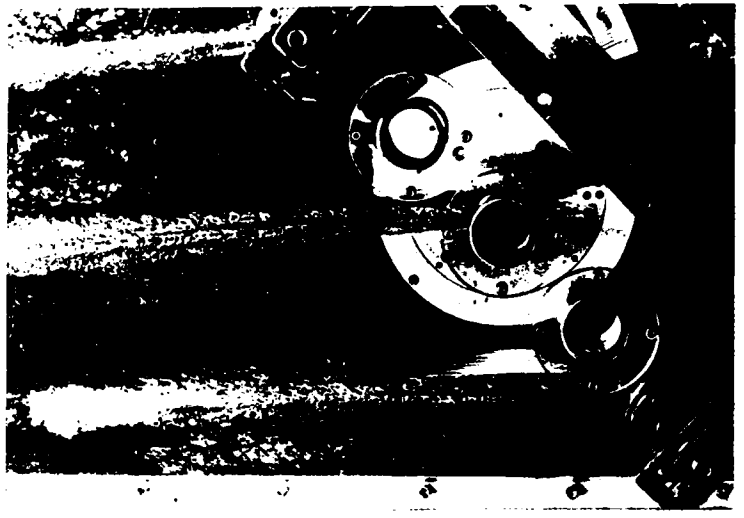

(d) σ = .18

FIGURE 10

Photographs of cavitation for sol = .5
α = 4°

(a) σ = .89

(b) σ = .49

(c) σ = .38

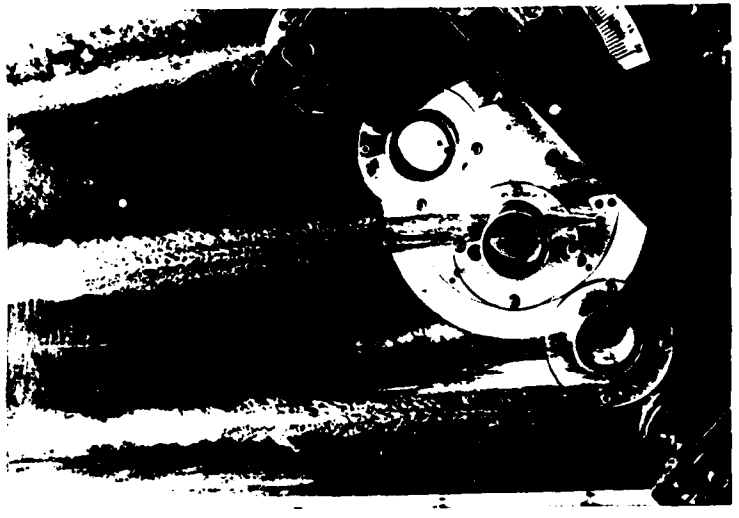

(d) σ = .22

FIGURE 11

Photographs of cavitation for sol = .5

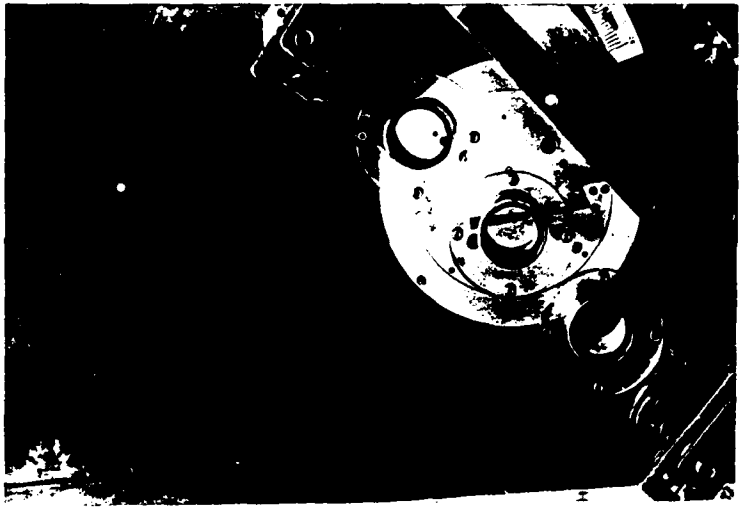

(a) σ = 1.04

(b) σ = .60

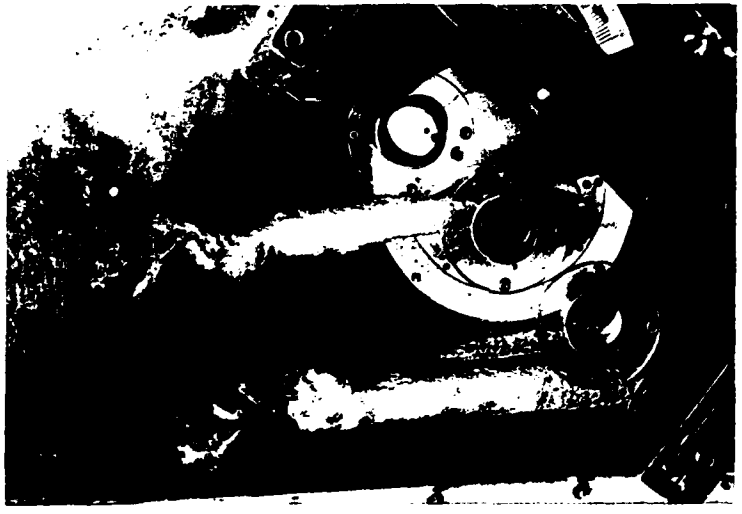

(c) σ = .32

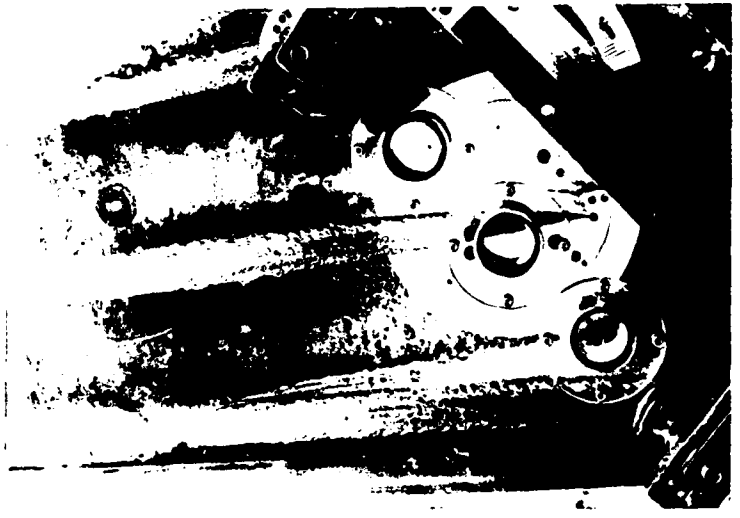

(d) σ = .30

FIGURE 12

Photographs of cavitation for sol = .5
α = 8°

(a) σ = .25

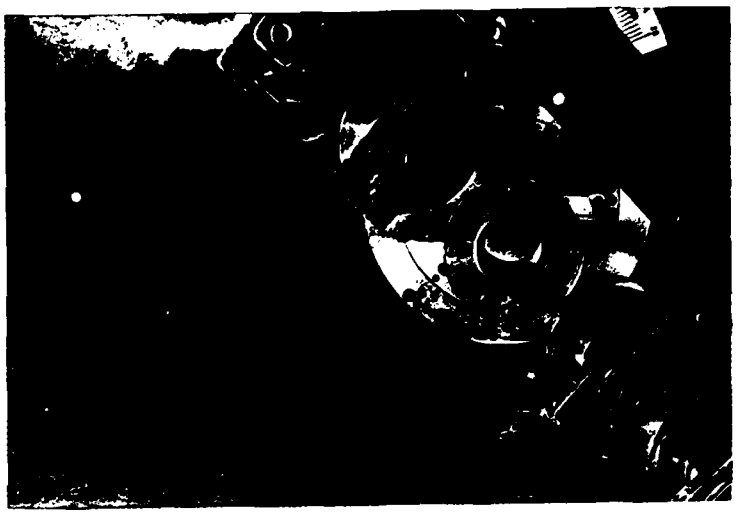

(b) σ = .22

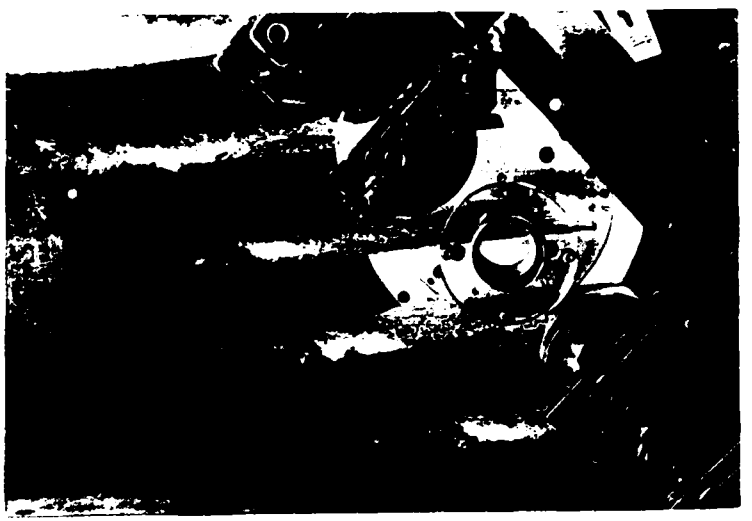

(c) σ = .20

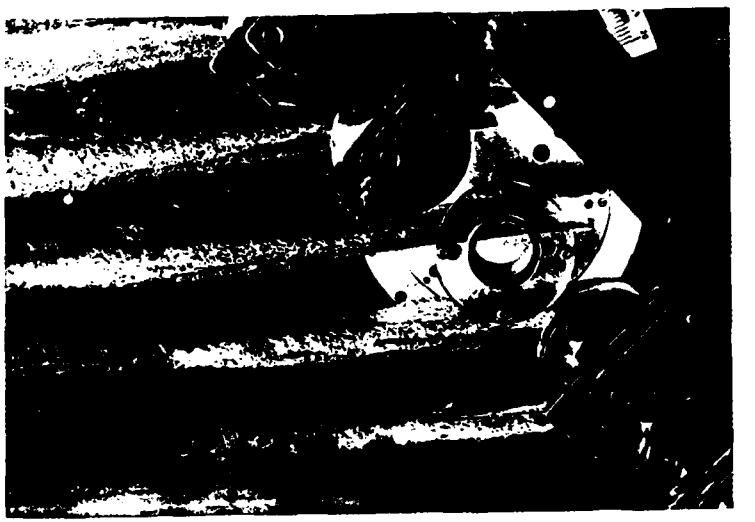

(d) σ = .17

FIGURE 13

Photographs of cavitation for sol = 1.0
α = 4°

(a) σ = .47

(b) σ = .40

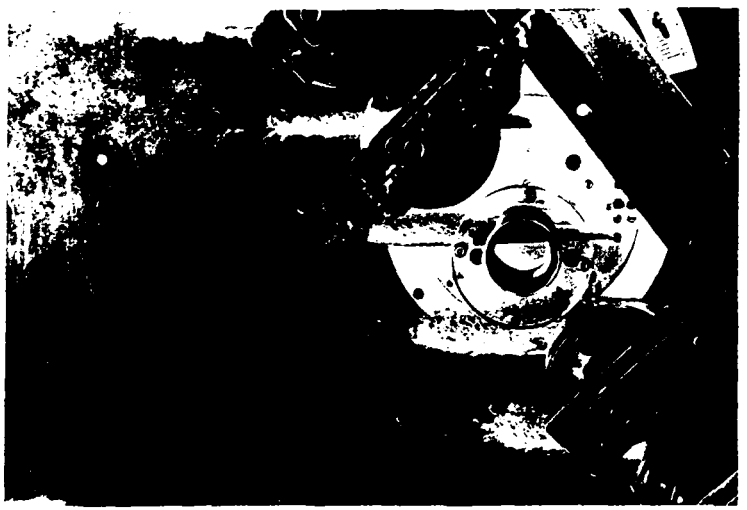

(c) σ = .27

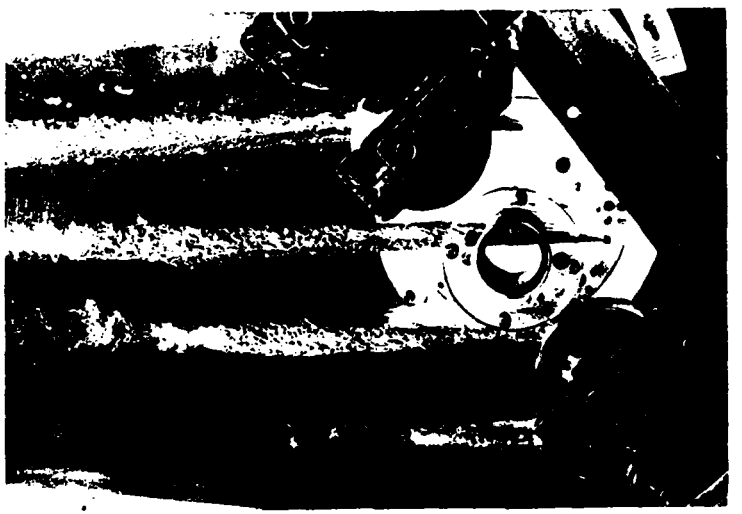

(d) σ = .22

FIGURE 14

Photographs of cavitation sol = 1.0
α = 6°

(a) σ = .69

(b) σ = .42

(c) σ = .26

(d) σ = .25

FIGURE 15

Photographs of cavitation for sol = 1.0
α = 8°

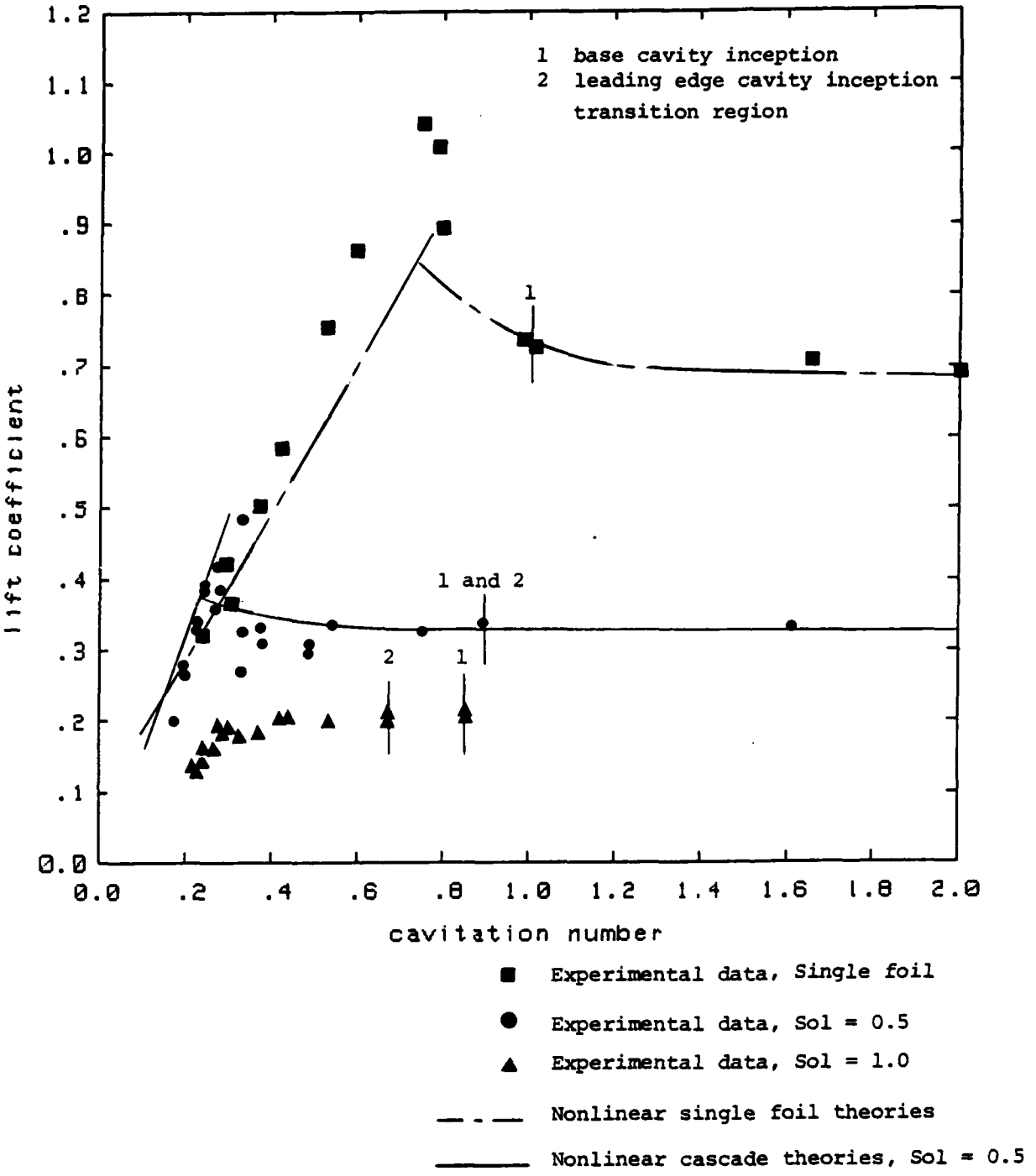

FIGURE 16

Lift coefficient vs. cavitation number
for $\alpha = 4°$

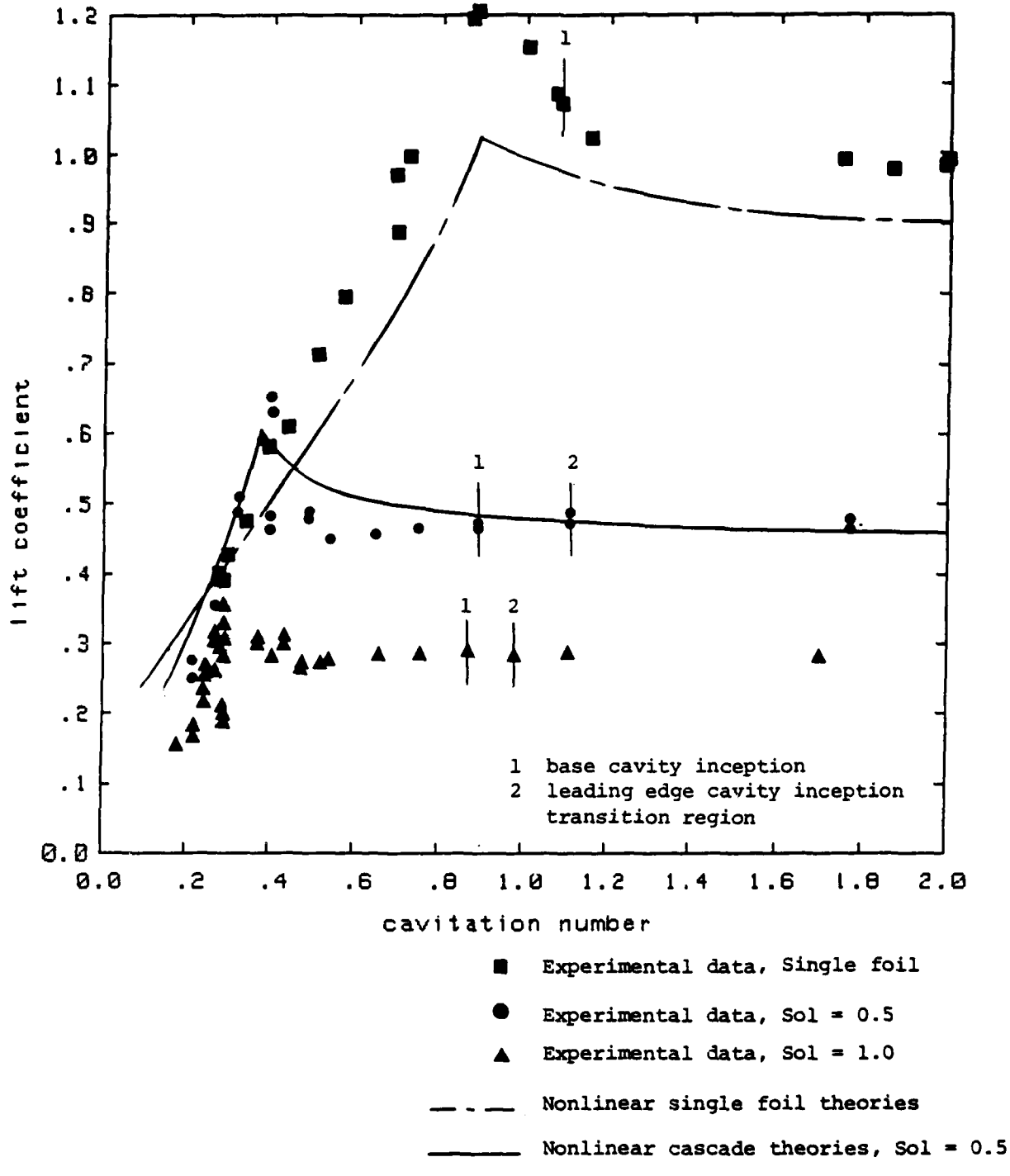

FIGURE 17

Lift coefficient vs. cavitation number
for $\alpha = 6°$

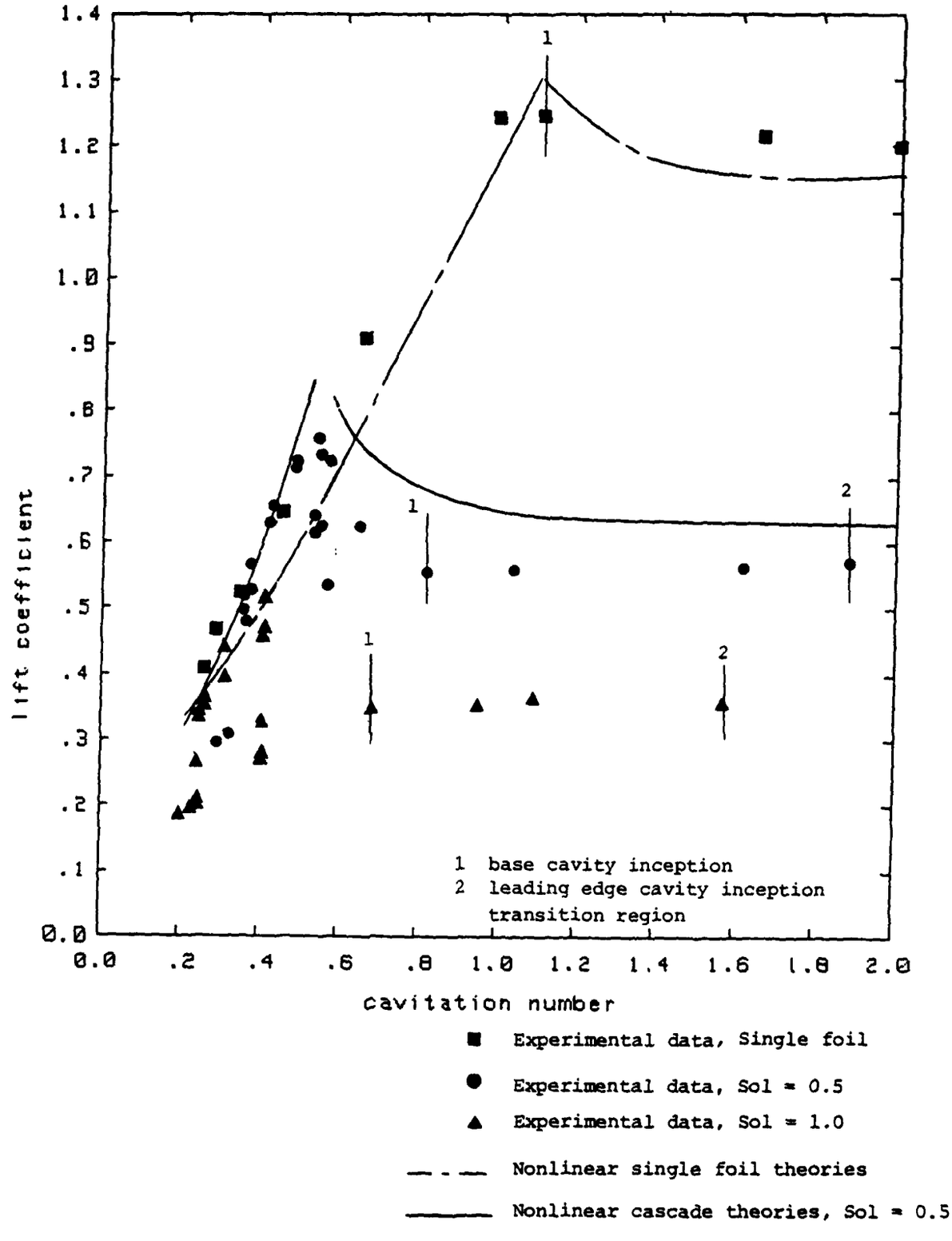

FIGURE 18

Lift coefficient vs. cavitation number
for $\alpha = 8°$

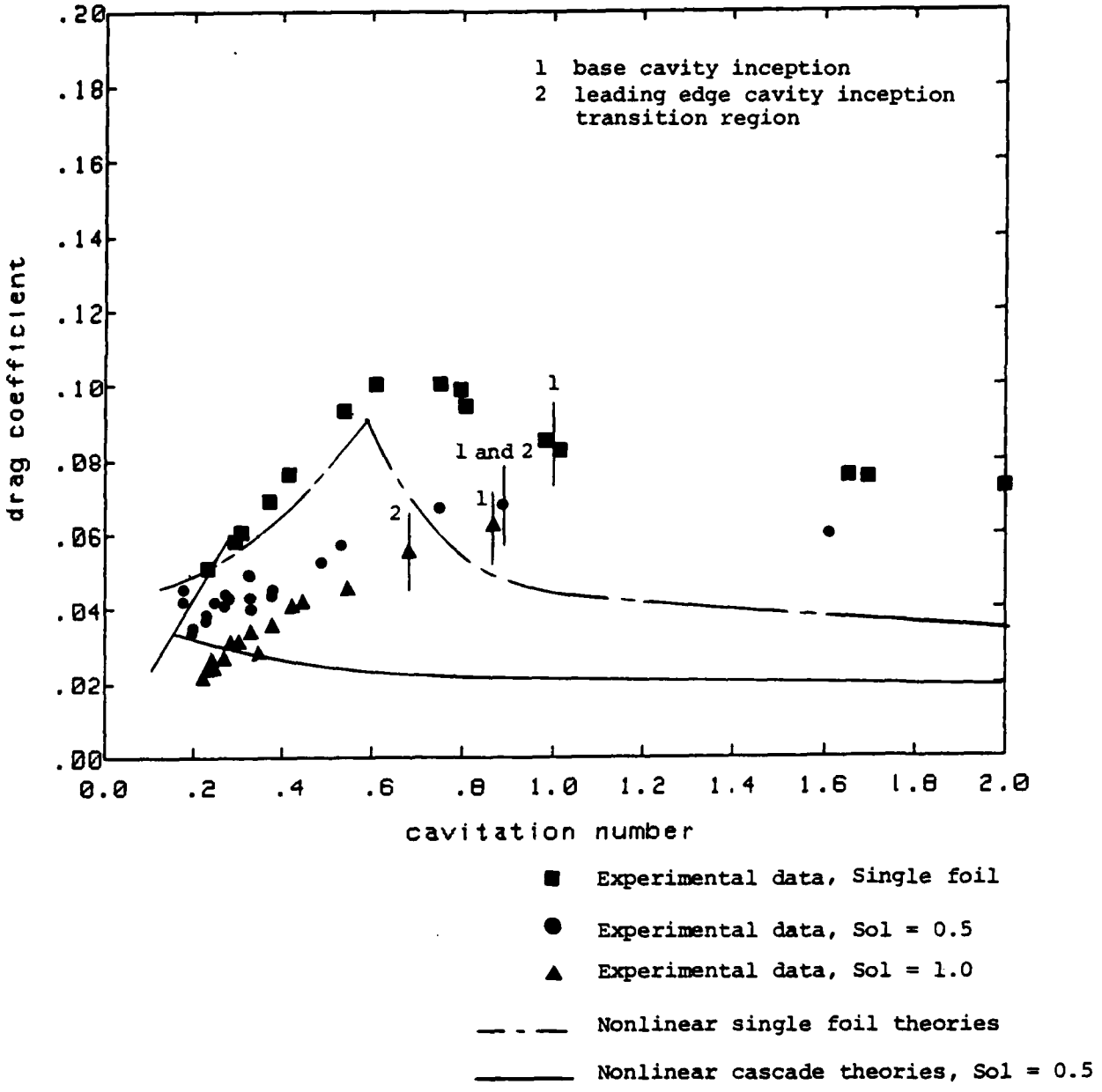

FIGURE 19

Drag coefficient vs. cavitation number
for $\alpha = 4°$

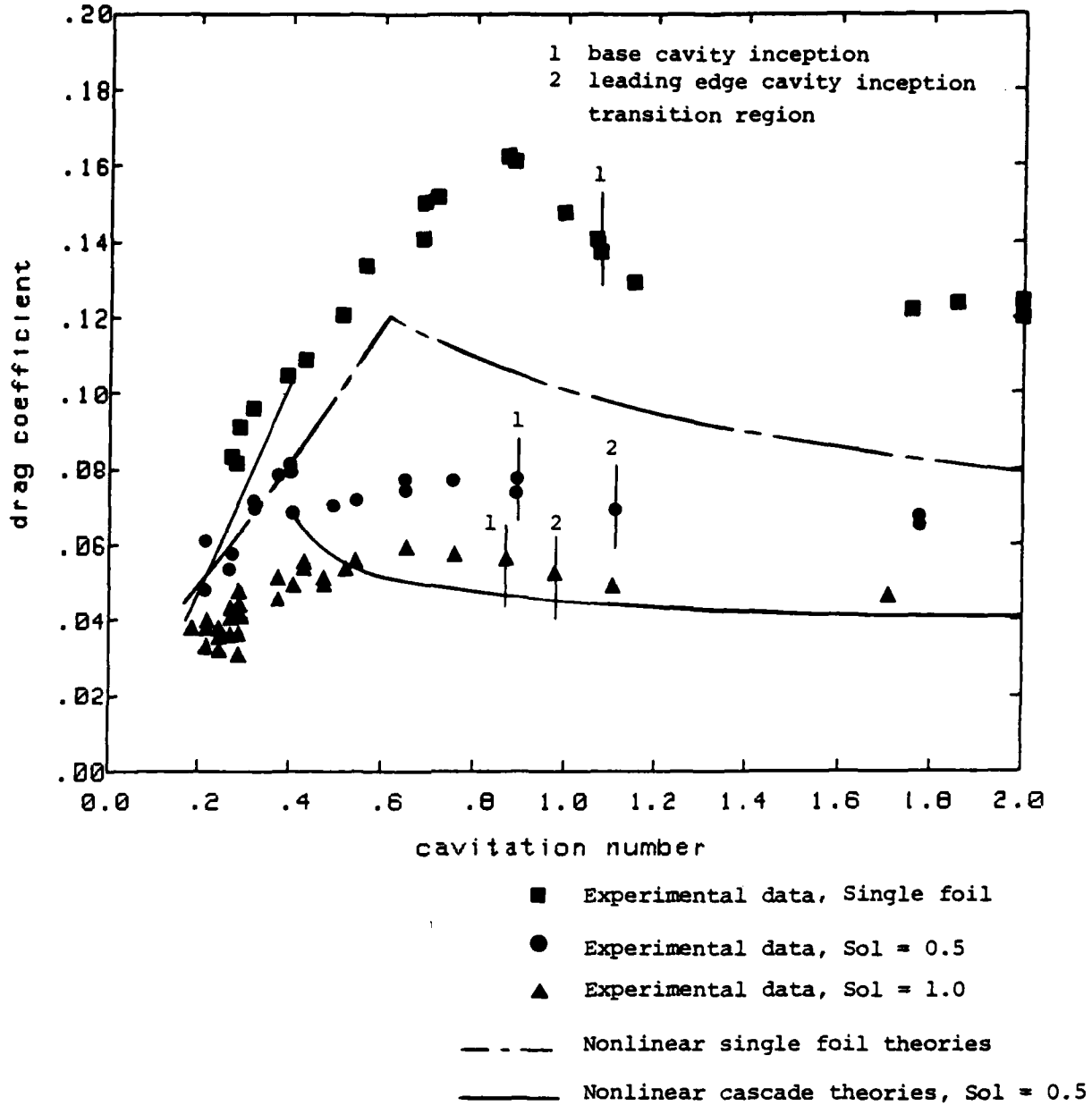

FIGURE 20

Drag coefficient vs. cavitation number
for $\alpha = 6°$

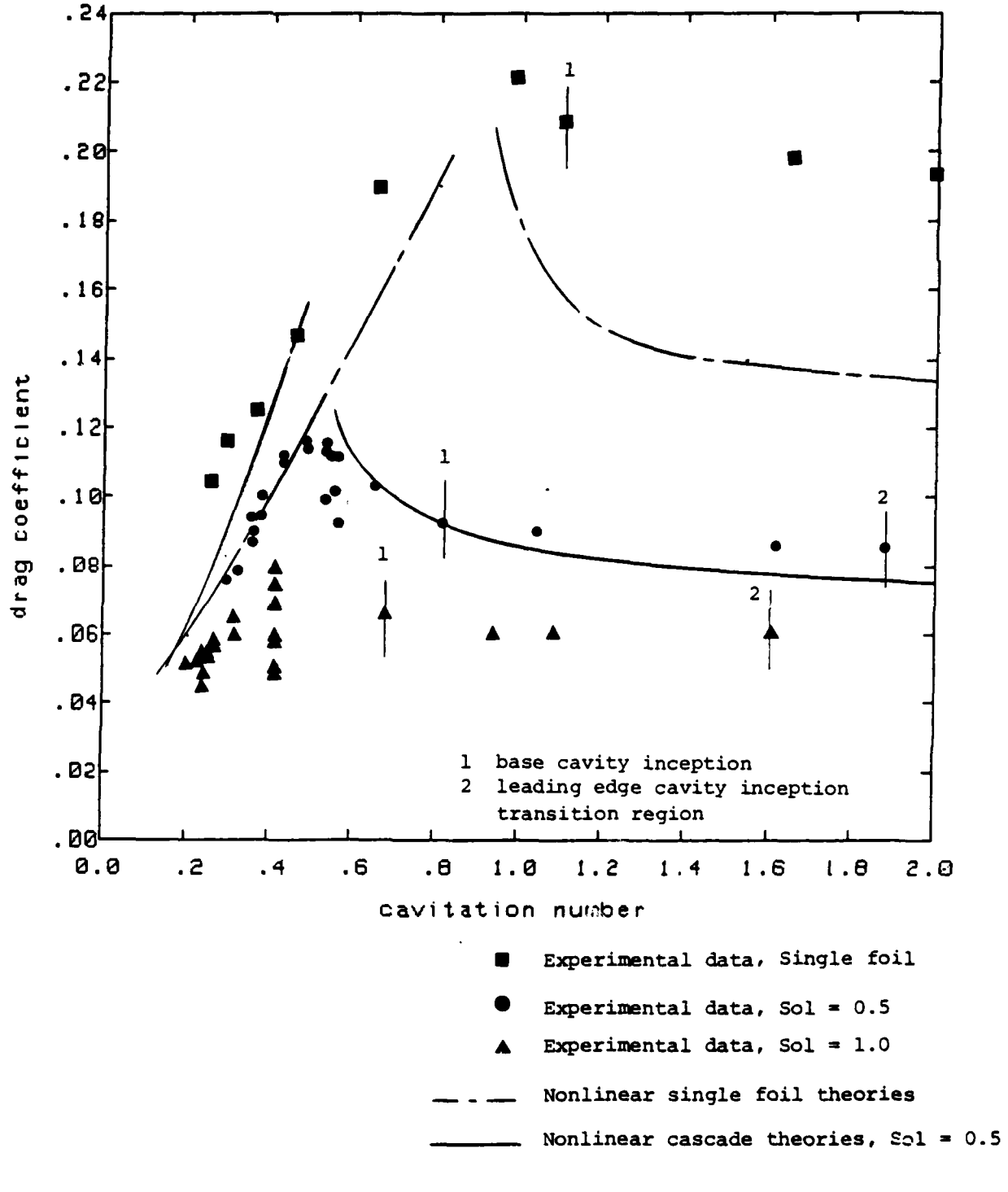

FIGURE 21

Drag coefficient vs. cavitation number
for $\alpha = 8°$

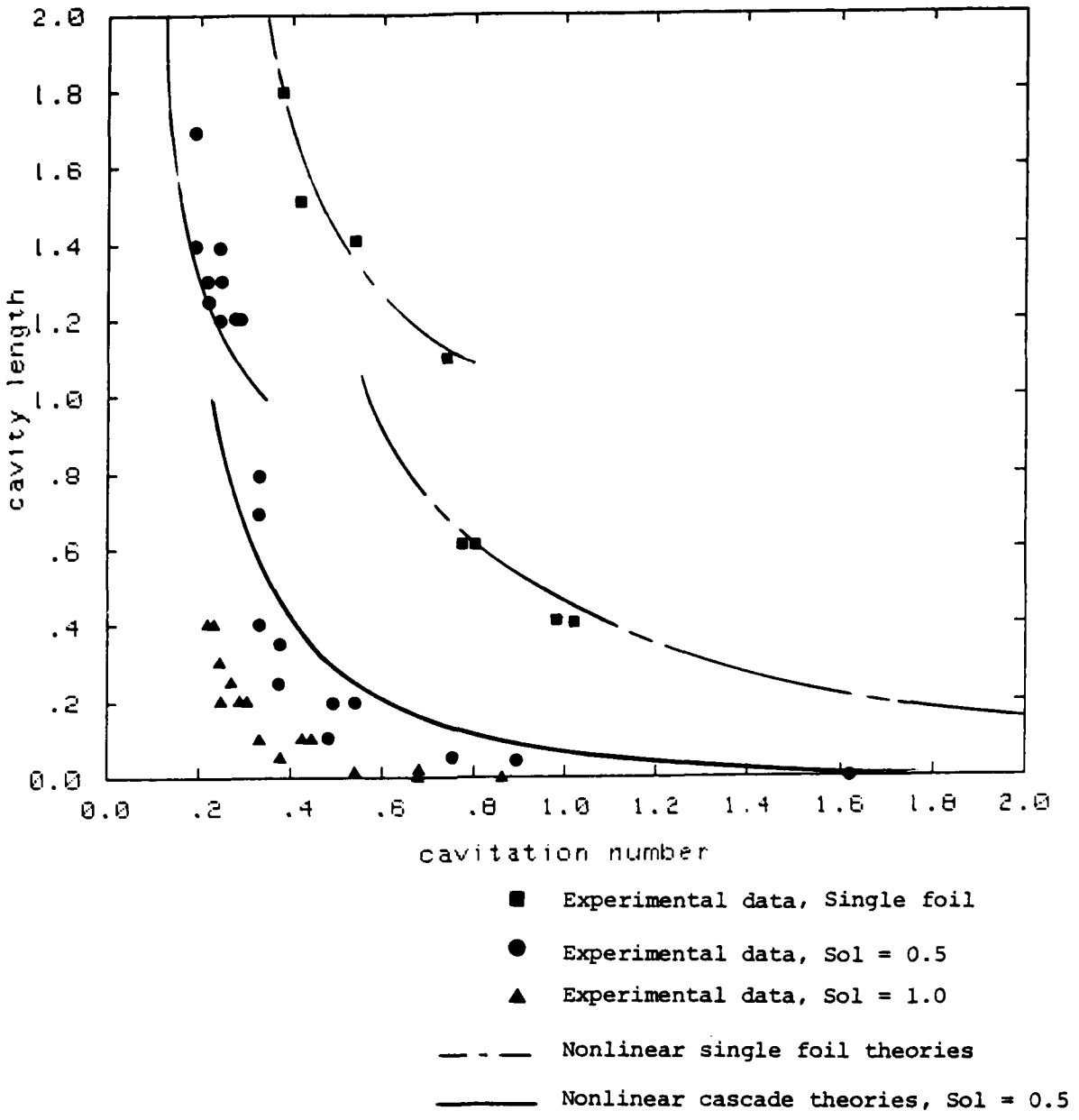

FIGURE 22

Cavity length vs. cavitation number
for $\alpha = 4°$

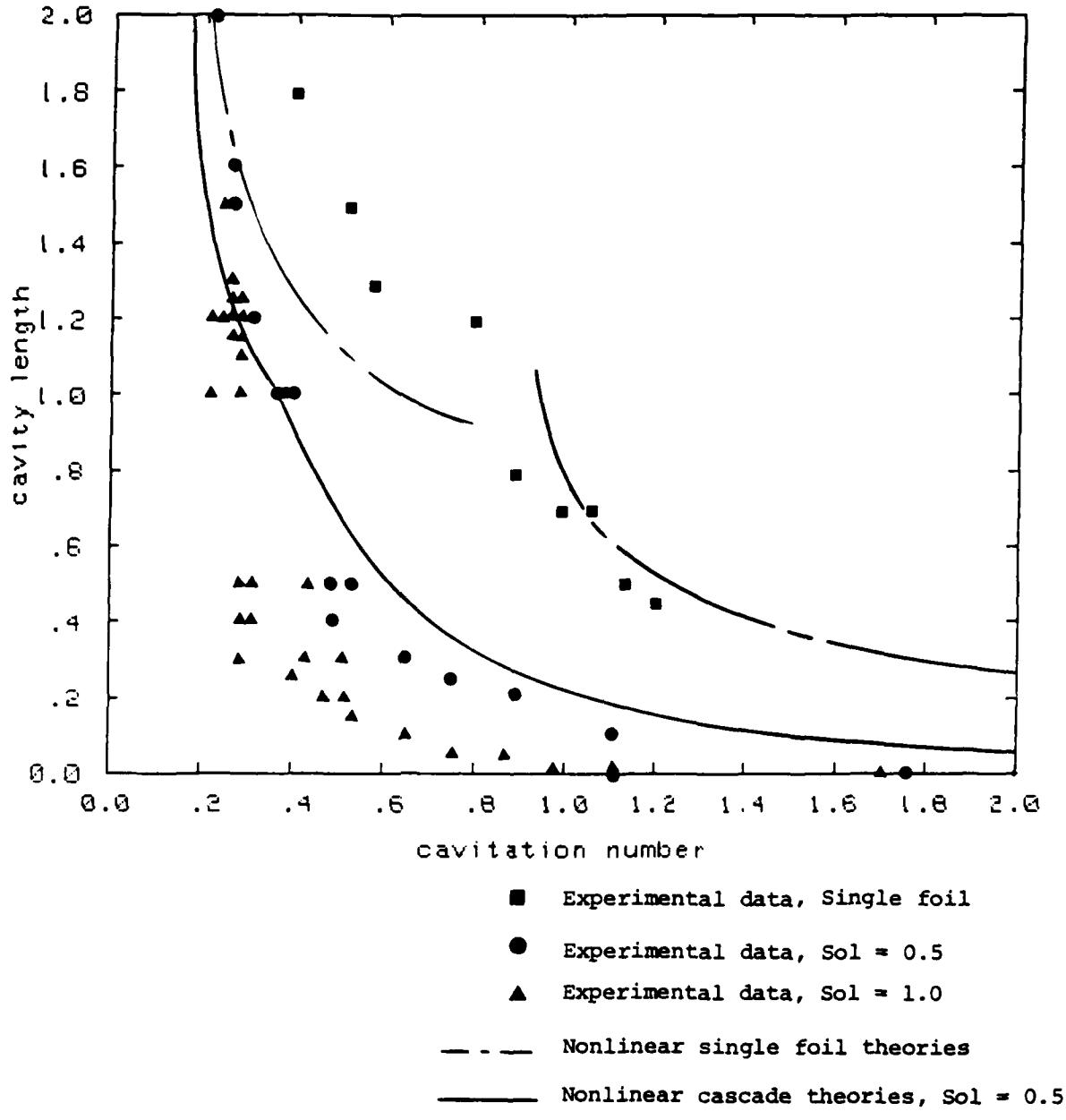

FIGURE 23

Cavity length vs. cavitation number
for $\alpha = 6°$

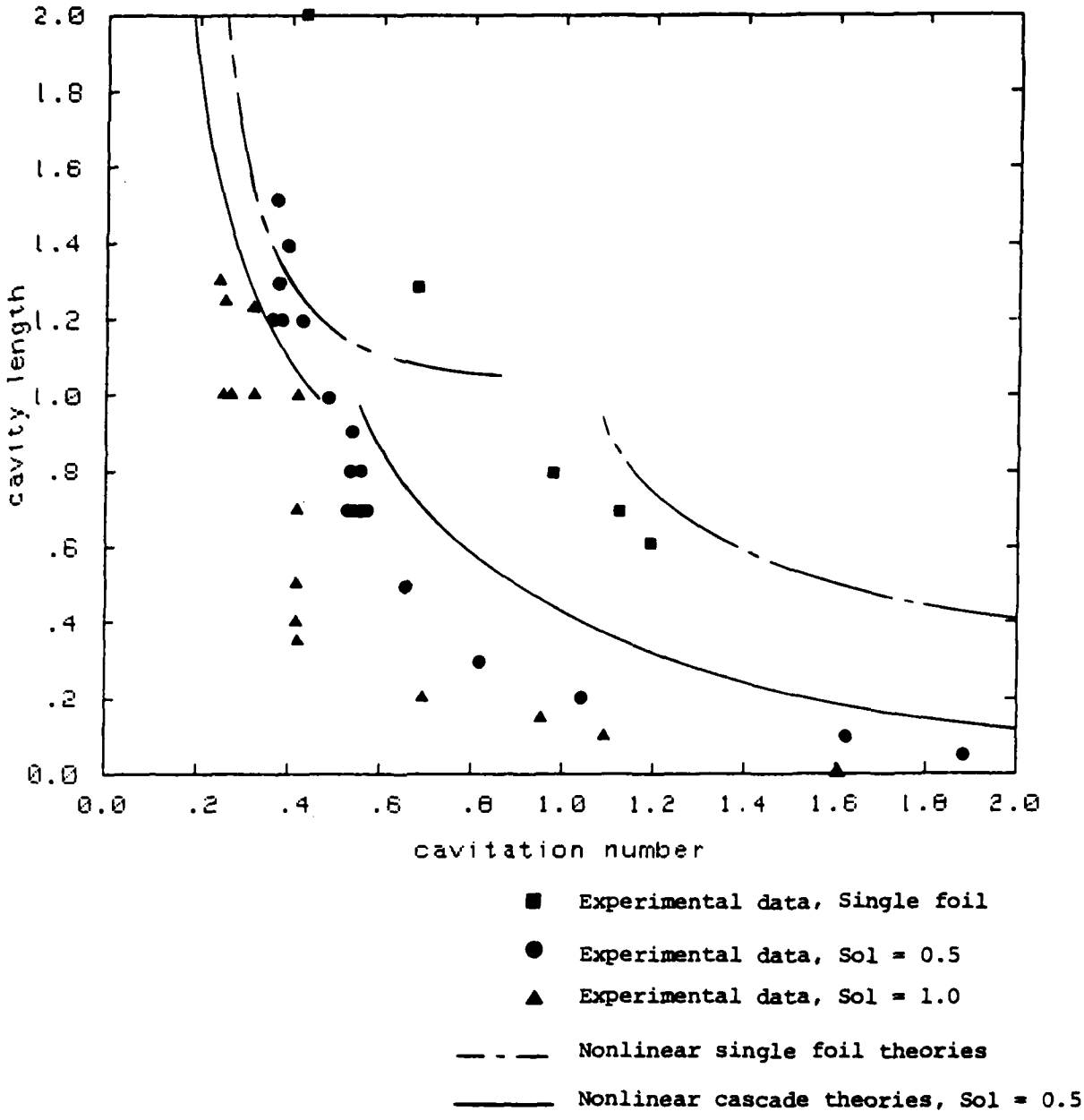

FIGURE 24

Cavity length vs. cavitation number
for $\alpha = 8°$

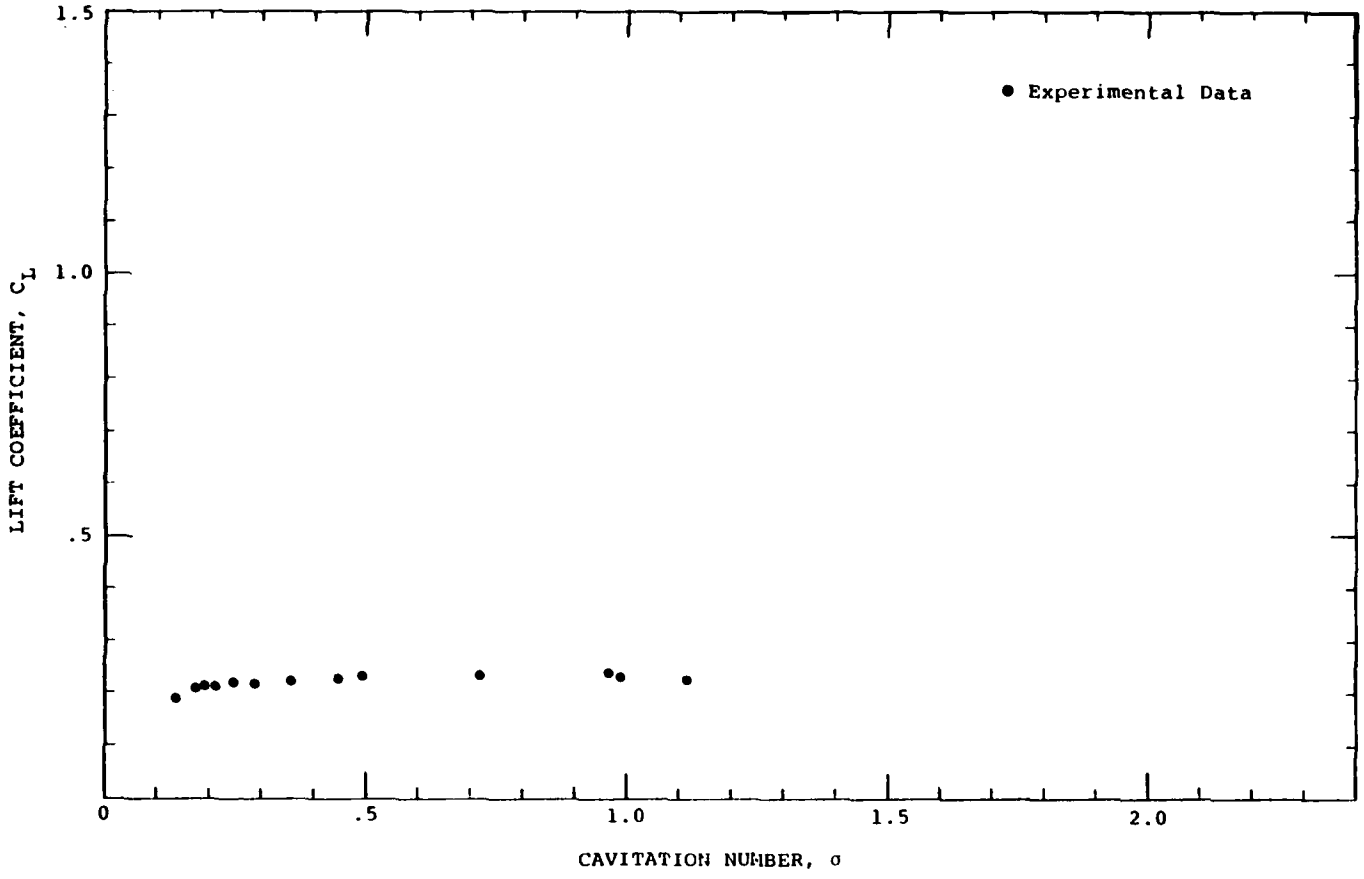

FIGURE 25

Lift coefficient of single foil at $\alpha = 0°$ as a function of cavitation number

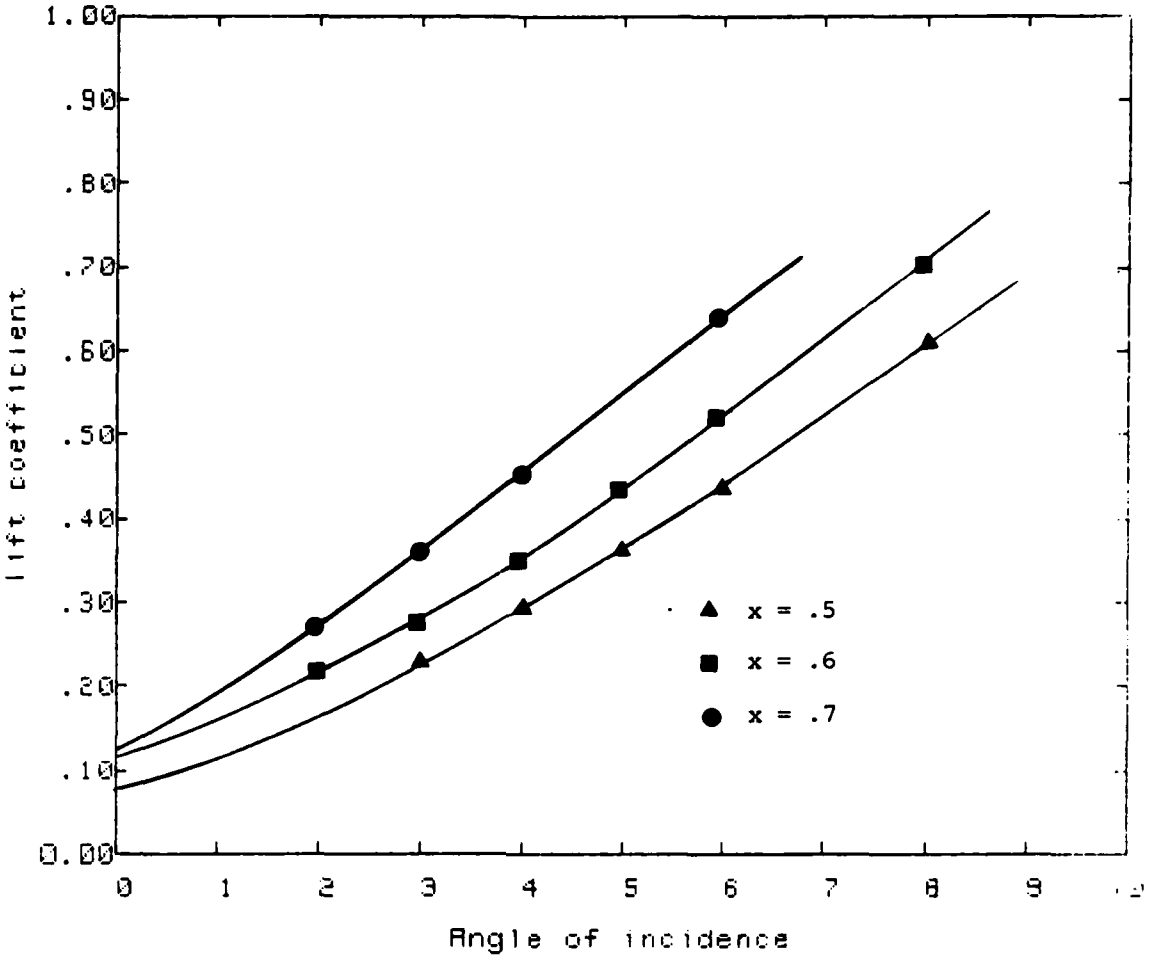

FIGURE 26

Extrapolations of lift coefficient at x = 0.5, 0.6 and 0.7 of Hydronautics' 7607.02 propeller at ℓ_c = 0.1

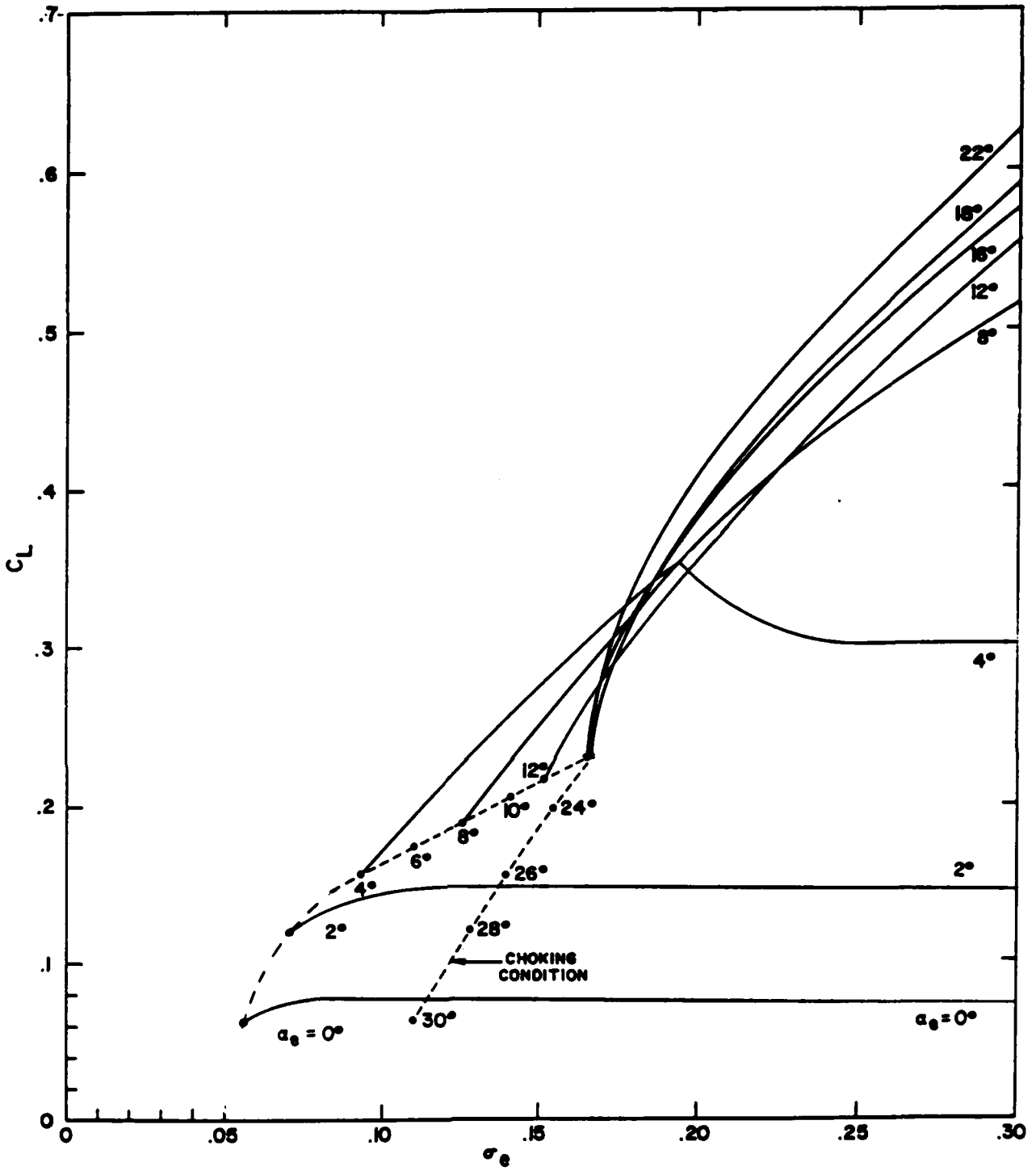

FIGURE 27

C_L vs. σ at x = .5 of
Hydronautics' 7607.02 propeller
used as an input of SCPROP2

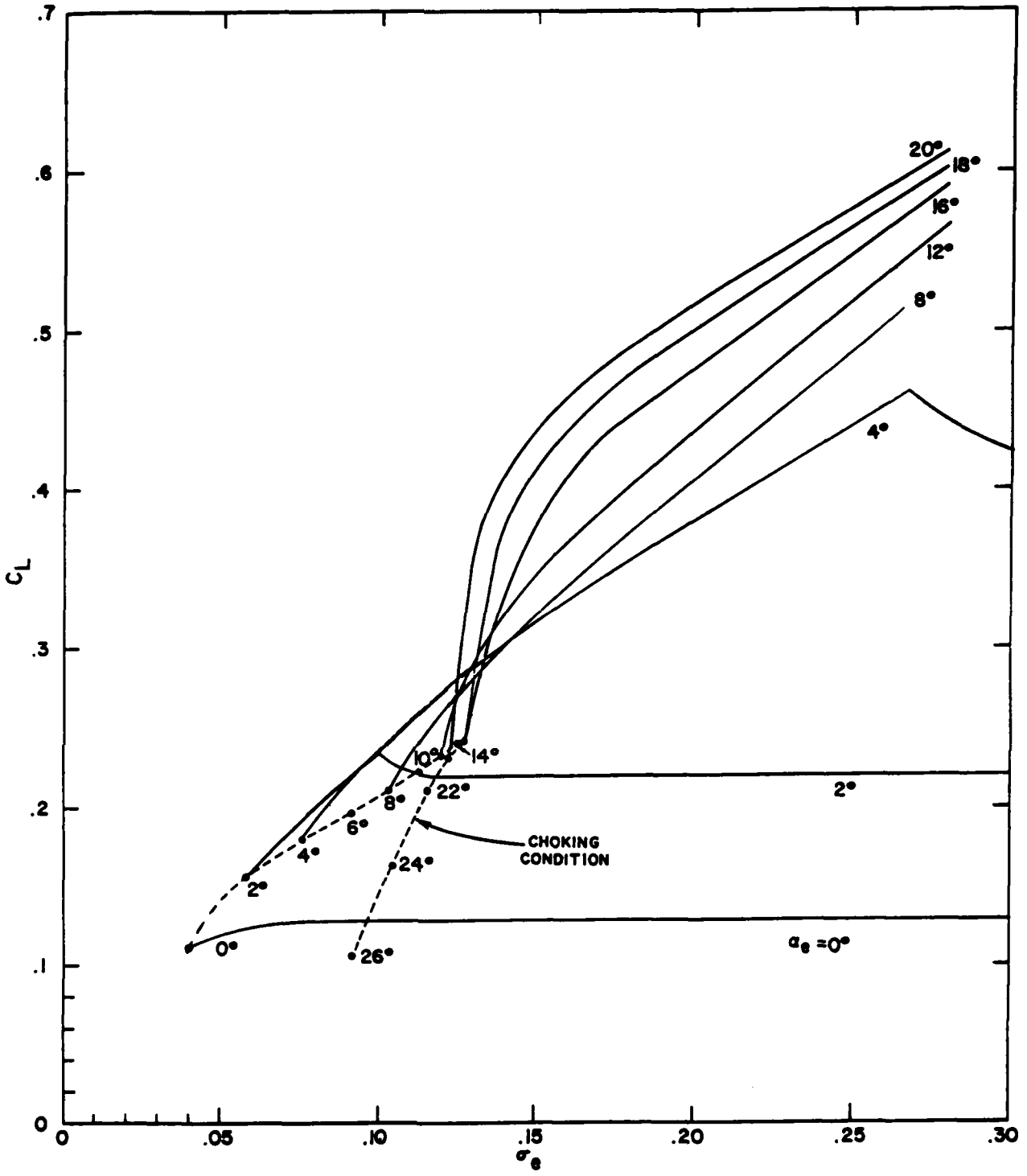

FIGURE 28

C_L vs. σ at x = .6 of
Hydronautics' 7607.02 propeller
used as an input of SCPROP2

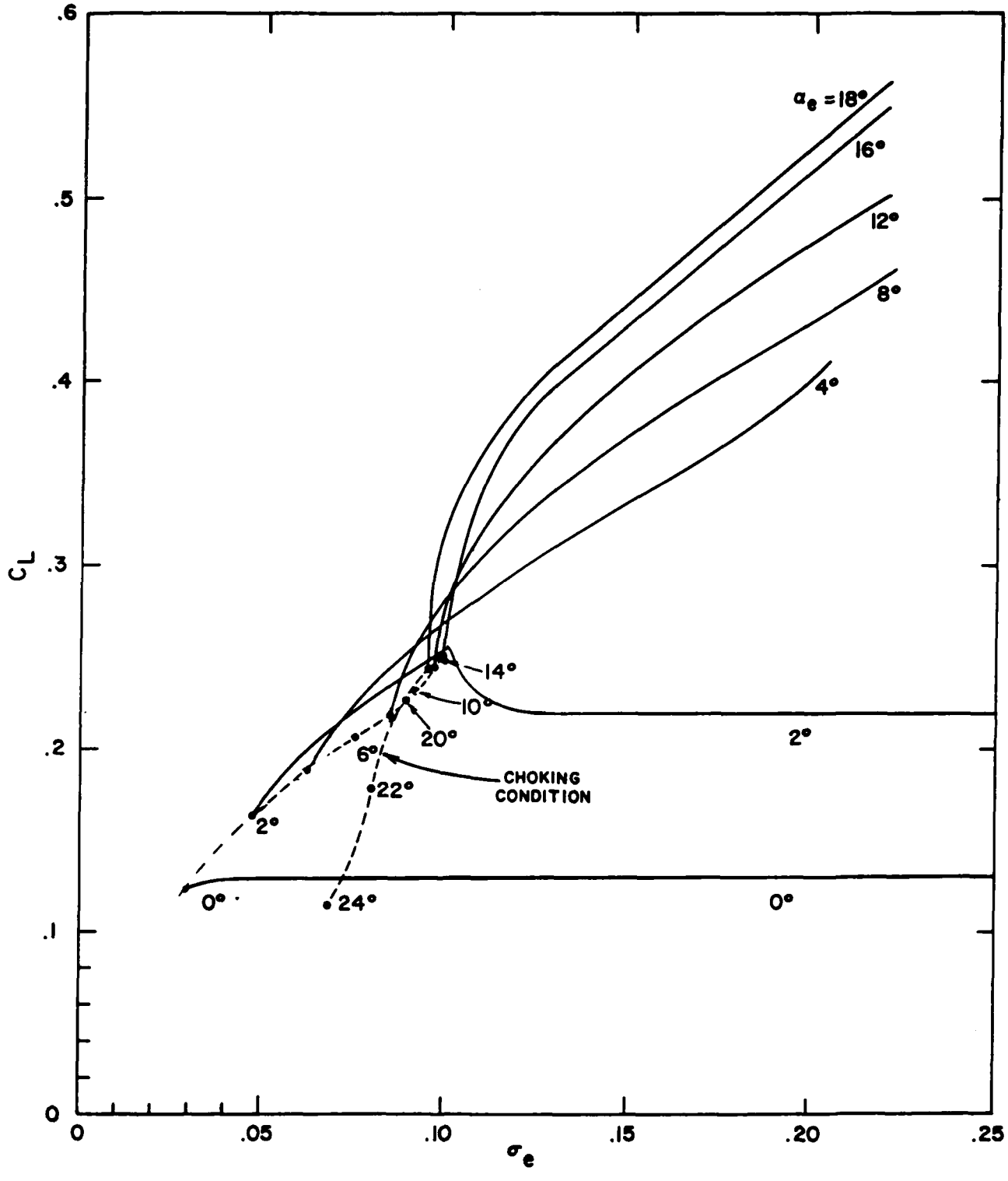

FIGURE 29

C_L vs. σ at x = .7 of
Hydronautics' 7607.02 propeller
used as an input of SCPROP2

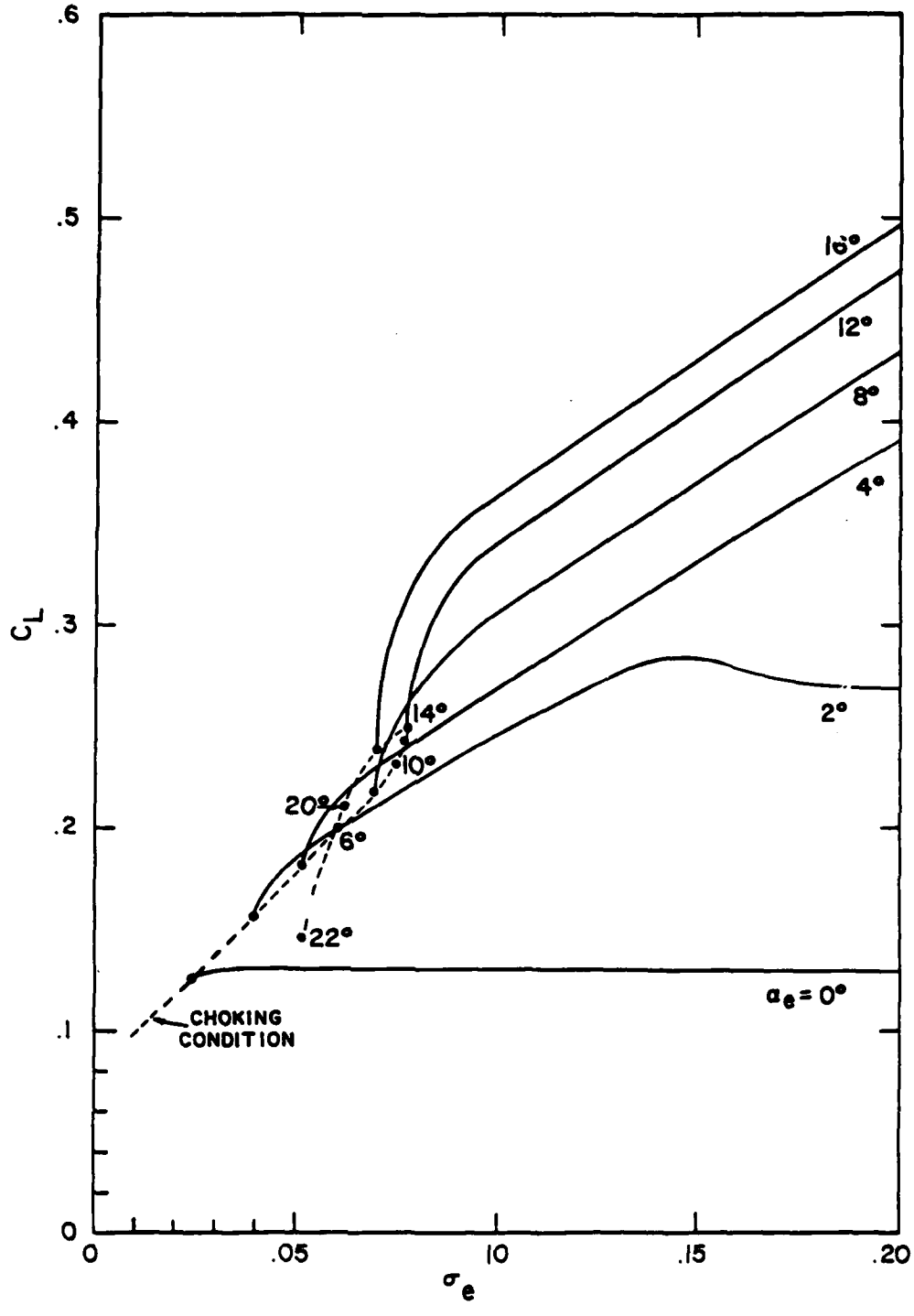

FIGURE 30

C_L vs. σ at x = .8 of
Hydronautics' 7607.02 propeller
used as an input of SCPROP2

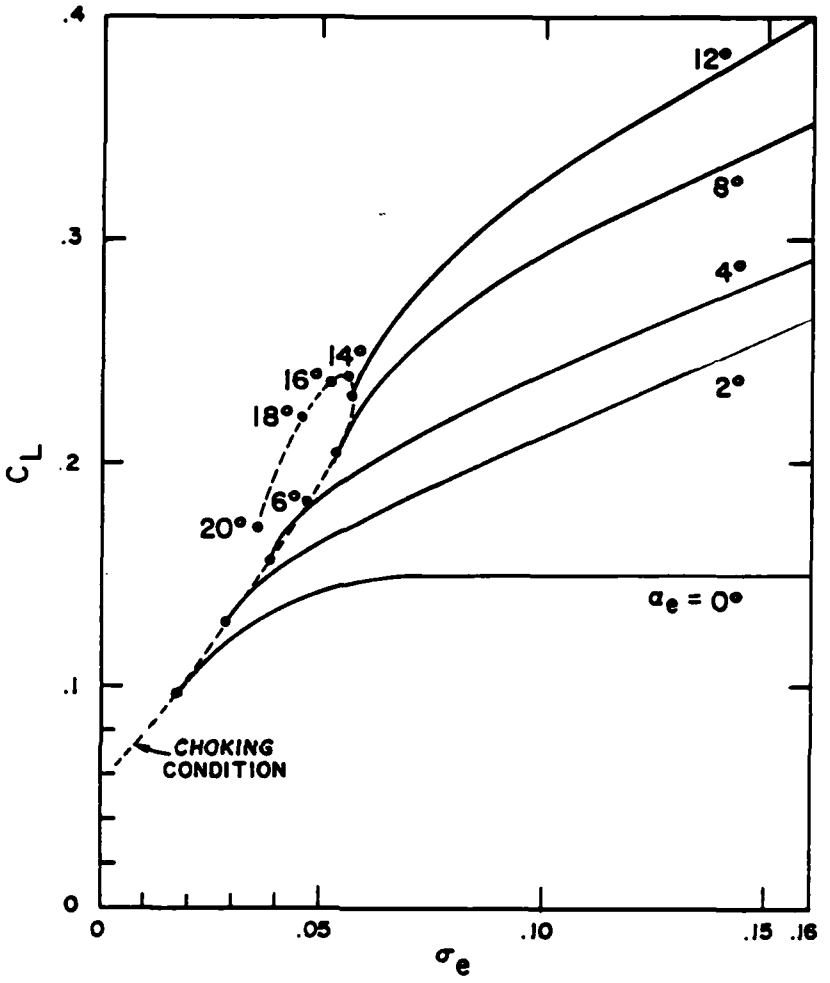

FIGURE 31

C_L vs. σ at x = .9 of
Hydronautics' 7607.02 propeller
used as an input of SCPROP2

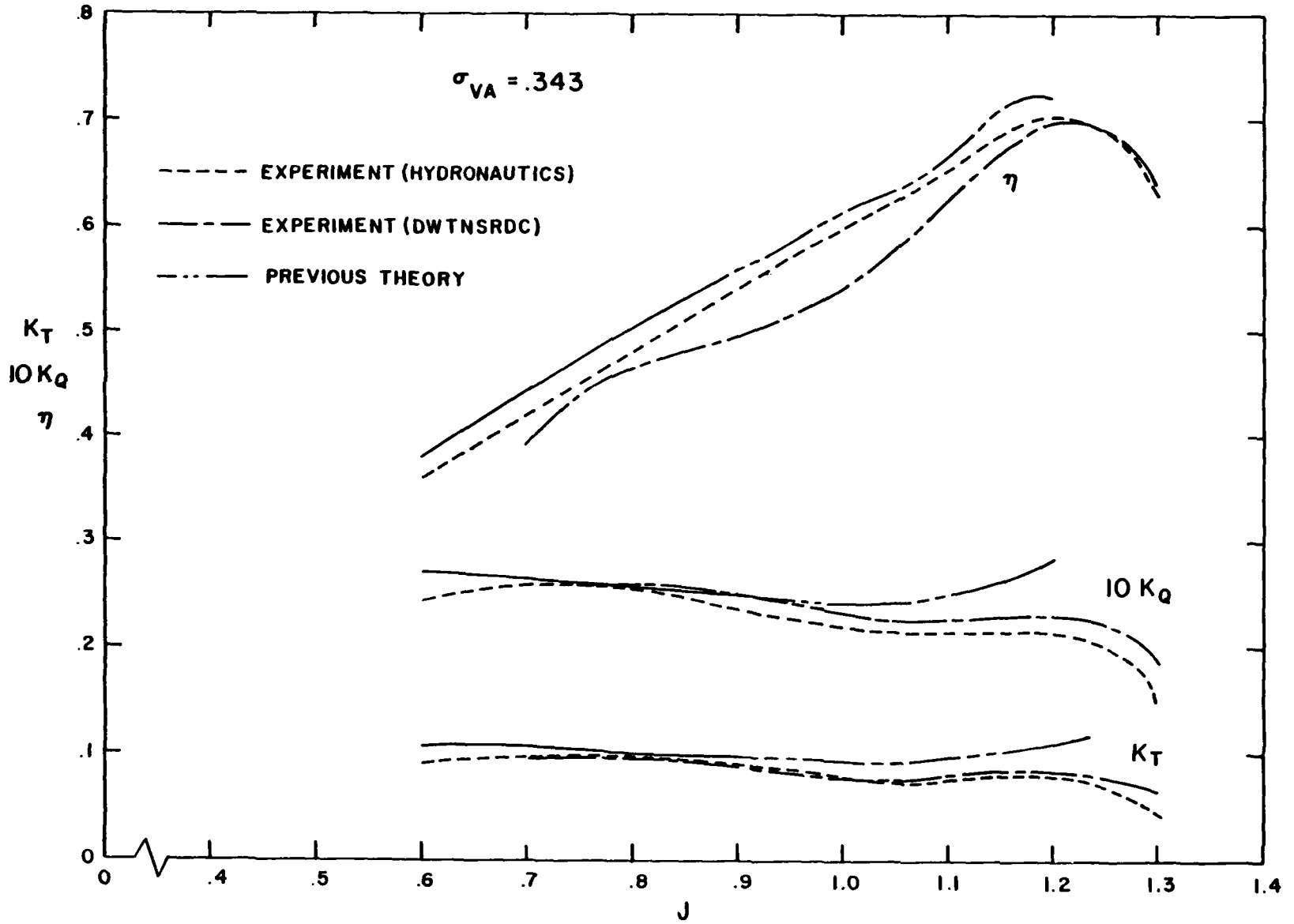

FIGURE 32

Comparison of the previous theory for K_T, K_Q and η of Hydronautics' 7607.02 at σ_V = .343 and experiments (Bohn 1977 and Peck 1977)

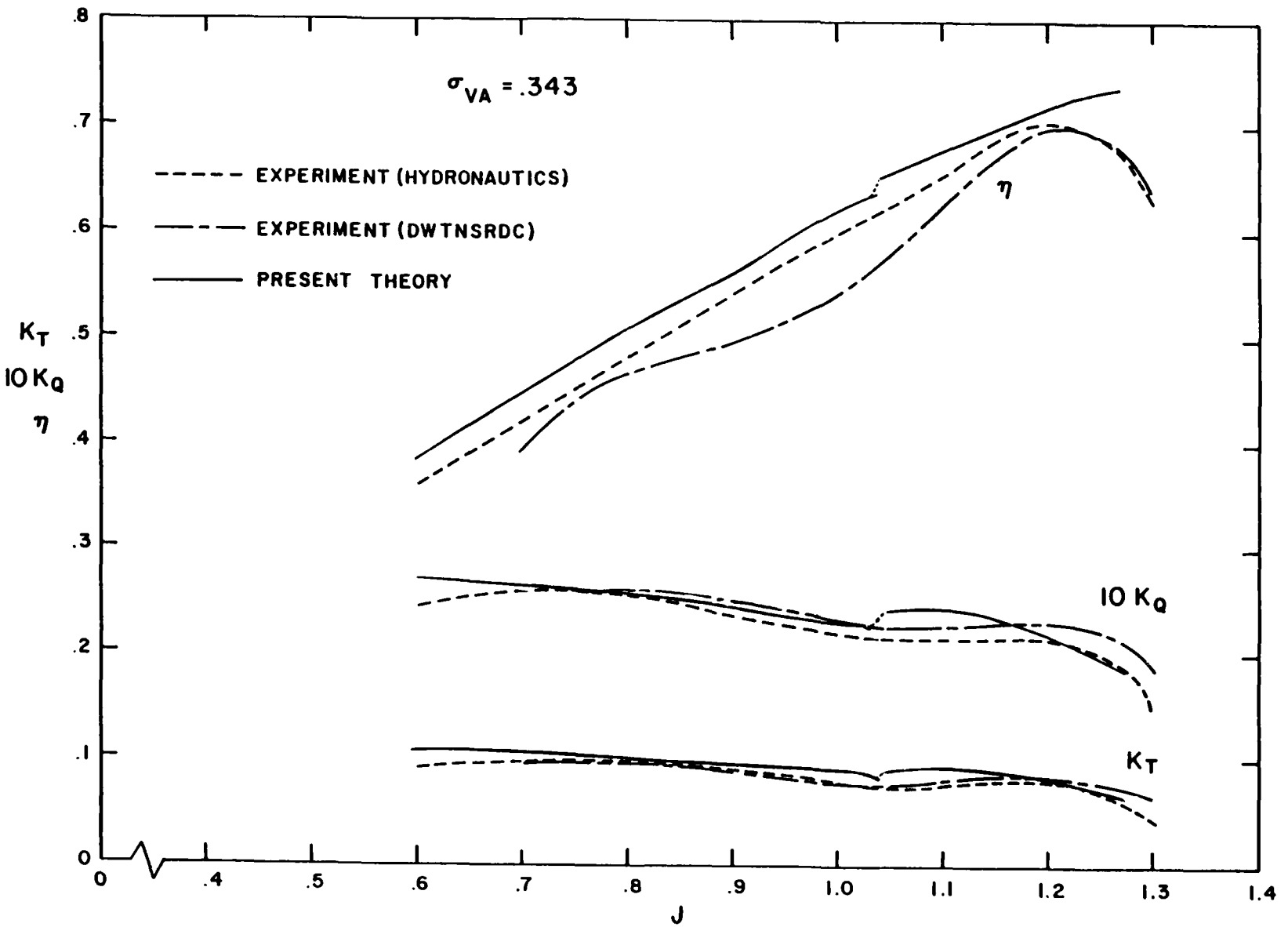

FIGURE 33

Comparison of the present results for K_T, K_Q and η of Hydronautics' 7607.02 at σ_V = .343 and experiments (Bohn 1977 and Peck 1977)

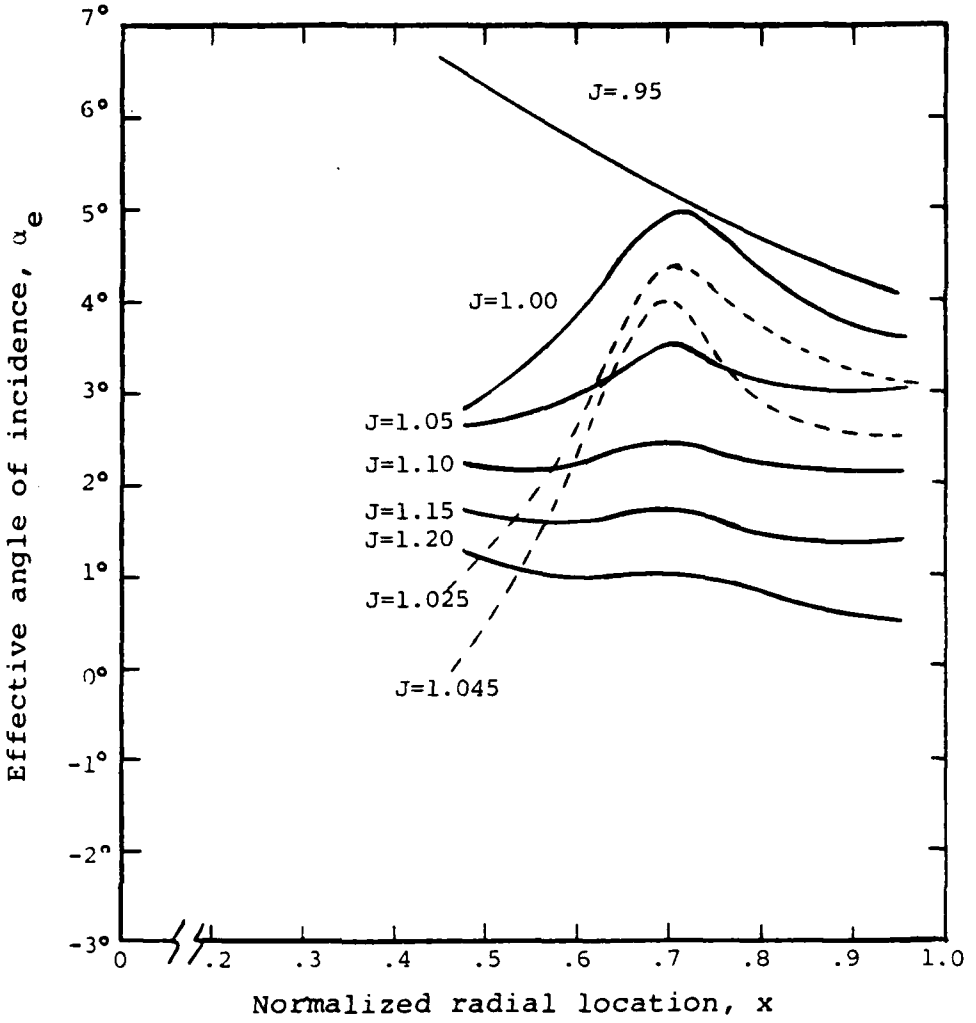

FIGURE 34

Local effective angle of incidence calculated by SCPROP2 at various J for Hydronautics' 7607.02

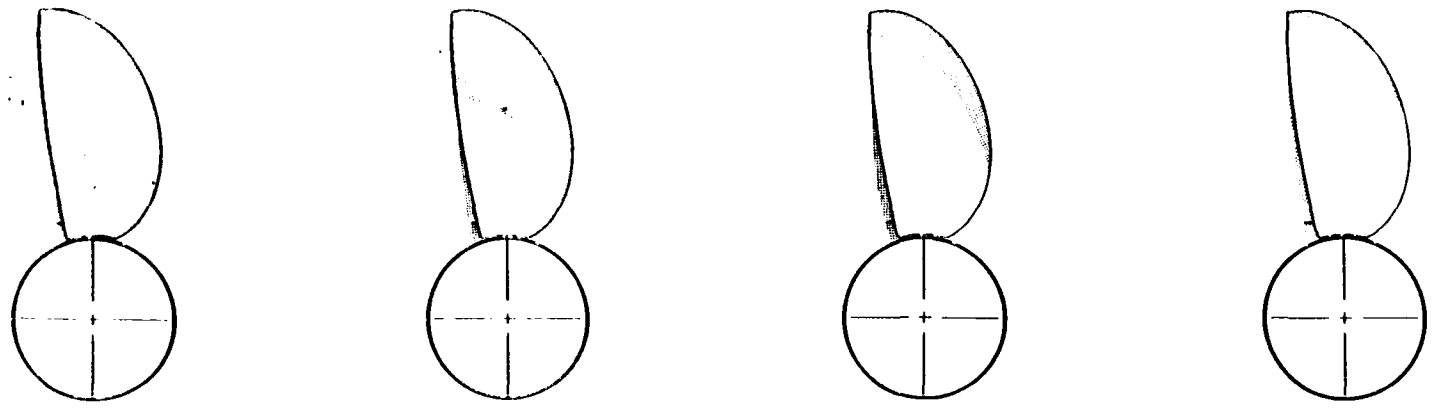

(a) Cavity envelopes observed in the experiment by Hydronautics

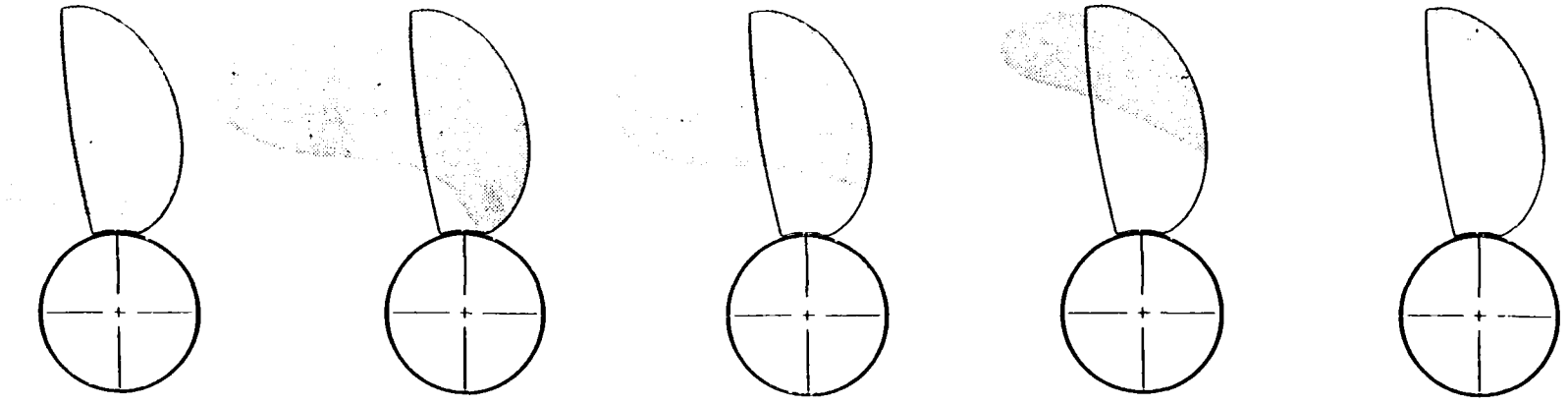

(b) Cavity envelopes predicted by SCPROP2

FIGURE 35

Cavity shape comparison of the present results and experimental observation by Bohn (1977) for Hydronautics' 7607.02 at σ_{V_a} = .343

END

DATE
FILMED

9 — 83

DTIC